

Planetesimal disk evolution driven by embryo-planetesimal gravitational scattering.

R. R. Rafikov

Princeton University Observatory, Princeton, NJ 08544

`rrr@astro.princeton.edu`

ABSTRACT

The process of gravitational scattering of planetesimals by a massive protoplanetary embryo is explored theoretically. We propose a method to describe the evolution of the disk surface density, eccentricity, and inclination caused by the embryo-planetesimal interaction. It relies on the analytical treatment of the scattering in two extreme regimes of the planetesimal epicyclic velocities: shear-dominated (dynamically “cold”) and dispersion-dominated (dynamically “hot”). In the former, planetesimal scattering can be treated as a deterministic process. In the latter, scattering is mostly weak because of the large relative velocities of interacting bodies. This allows one to use the Fokker-Planck approximation and the two-body approximation to explore the disk evolution. We compare the results obtained by this method with the outcomes of the direct numerical integrations of planetesimal orbits and they agree quite well. In the intermediate velocity regime an approximate treatment of the disk evolution is proposed based on interpolation between the two extreme regimes. We also calculate the rate of embryo’s mass growth in an inhomogeneous planetesimal disk and demonstrate that it is in agreement with both the simulations and earlier calculations. Finally we discuss the question of the direction of the embryo-planetesimal interaction in the dispersion-dominated regime and demonstrate that it is repulsive. This means that the embryo always forms a gap in the disk around it, which is in contrast with the results of other authors. The machinery developed here will be applied to realistic protoplanetary systems in future papers.

Subject headings: planets and satellites: general — solar system: formation — (stars:) planetary systems

1. Introduction.

This paper continues the line of investigation started in our previous work (Rafikov 2001, 2002a; hereafter Papers I and II) which was devoted to the treatment of planetesimal-planetesimal gravitational interactions. Here we consider the interaction between the growing protoplanetary

embryo and the planetesimal disk. By embryo we imply in the present context a single body with mass M_e much larger than the masses of individual planetesimals m . There are several reasons for studying this important problem separately from the mutual gravitational scattering of planetesimals.

First, planetesimal-planetesimal encounters in realistic protoplanetary disks usually occur in the dispersion-dominated regime, which applies when the relative approach velocity of two particles is bigger than the differential shear in the disk across the Hill (or tidal) radius. The Hill radius is defined as

$$r_H = a \left(\frac{m_1 + m_2}{M_c} \right)^{1/3}, \quad (1)$$

where a is a value of the semimajor axis at which the interaction takes place, and m_1, m_2 , and M_c are the masses of interacting planetesimals and of the central star.

However, in the same protoplanetary disk gravitational interaction between the embryo and planetesimals could be in the opposite velocity regime — shear-dominated — when the planetesimal random motion is small compared to the shear across the Hill radius, simply because the embryo mass and therefore the Hill radius is much larger. Indeed, in the case of embryo-planetesimal interactions Hill radius $R_H = a_e(M_e/M_c)^{1/3} \gg r_H$ (here a_e is a semimajor axis of the embryo) as a consequence of $M_e \gg m_i$. Thus, reduced (normalized in Hill coordinates) values of random velocities in the embryo-planetesimal case are smaller by a factor $[(m_1 + m_2)/M_e]^{1/3} \ll 1$ than those corresponding to the planetesimal-planetesimal interactions.

Of course, it might be that the planetesimal disk has already been so excited dynamically that even embryo-planetesimal encounters are in the dispersion-dominated regime. Thus, we consider here both regimes of the embryo-planetesimal interaction — shear- and dispersion-dominated.

Second, embryo-planetesimal interactions are complicated by the presence of a special type of orbits in a 3-body problem — the so-called horseshoe (or librating) orbits (Hénon & Petit 1986; Murray & Dermott 1999). Planetesimals on these orbits do not perform the usual circulating motion which is characteristic of passing orbits (the most important case for planetesimal-planetesimal scattering) but a librating one. This horseshoe motion can only occur when the difference in semimajor axes of interacting bodies is smaller than their Hill radius. For planetesimal-planetesimal interactions r_H is negligible compared to the scale of surface density variations or the radial epicyclic excursion of an individual planetesimal. Thus horseshoe orbits are unimportant in this case. However, the Hill radius of the embryo-planetesimal interaction R_H can be comparable to the length scale of the disk inhomogeneities caused by the embryo. Thus the phenomenon of horseshoe motion can be crucial for the planetesimal dynamics near the embryo (see below §3.1).

Third, as we have already mentioned in Paper II, planetesimal-planetesimal scattering is described in terms of the disk properties *averaged* over some region of the disk, which diminishes the importance of the details of spatial distributions of disk properties. On the contrary, in the case of

the embryo-planetesimal interaction we are interested in details of the *spatial behavior* of various quantities characterizing the state of the disk and they are the primary goal of our present study.

All these complications preclude the direct application of the results obtained in Paper II to the present consideration. However the general analytical approach to the treatment of planetesimal disk evolution developed there remains valid and we will employ it in this paper.

Numerical orbit integrations (Tanaka & Ida 1996, 1997) and N-body simulations (Ida & Makino 1993) provide an alternative and important route of studying embryo-planetesimal interactions. Their drawback is their intrinsically low speed and inability to treat large number of planetesimals. However, since the physics is incorporated in them on a very basic level with the minimum of additional assumptions they can provide us with robust predictions. To use this advantage of numerical methods and to avoid their handicaps we employ the following methodology: we provide a self-consistent *analytical* description of the embryo-planetesimal interaction in different velocity regimes. To check this description and to verify the validity of the simplifying assumptions utilized in its development we have used numerical orbit integrations performed for several sets of typical planetesimal disk parameters. After we make sure that our theory works well for these sets of parameters we can use it for others as well and be confident of its reliability. What we gain by this approach is the speed of computation and ability to explore the whole space of important physical variables.

The condition on the embryo’s mass, $M_e \gg m$, has important dynamical implications. In many applications it justifies the neglect of the embryo’s recoil resulting from planetesimal scattering. Also, dynamical friction between the embryo and planetesimals will tend to produce random energy equipartition (Stewart & Wetherill 1988; Wetherill & Stewart 1989) which means that embryo’s eccentricity and inclination are most likely to be negligibly small. Thus, we will assume in this paper that the embryo moves on a fixed circular orbit and its eccentricity and inclination are zero. We will also consider the embryo to be isolated from the gravitational effects of other massive bodies which may be growing nearby, an assumption which can easily be abandoned in future work. Throughout the paper we neglect the presence of any resonant effects. This is justifiable if frequent planetesimal-planetesimal encounters can destroy any commensurabilities with the embryo’s rotation period. The embryo’s recoil in the course of planetesimal scattering and distant embryo-embryo interactions would also help to do that. We leave for the future the clarification of conditions necessary for employing this simplification.

It will be convenient to use the embryo’s Hill radius R_H as a unit of length in our study. We introduce the Hill orbital elements of a planetesimal evaluated at large azimuthal distance from the embryo — the difference in semimajor axes H , eccentricity \tilde{e} , and inclination \tilde{i} relative to the embryo’s orbit at semimajor axis a_e :

$$H = \frac{a - a_e}{R_H}, \quad \tilde{e} = e \frac{a_e}{R_H}, \quad \tilde{i} = i \frac{a_e}{R_H}, \quad (2)$$

and use them as planetesimal coordinates. The distribution function of the orbital elements \tilde{e} and

\tilde{i} will be assumed to have a Rayleigh form with dispersions $\tilde{\sigma}_e$ and $\tilde{\sigma}_i$:

$$\psi(\tilde{e}, \tilde{i}) d\tilde{e} d\tilde{i} = \frac{\tilde{e} d\tilde{e} \tilde{i} d\tilde{i}}{\tilde{\sigma}_e^2 \tilde{\sigma}_i^2} \exp \left[-\frac{\tilde{e}^2}{2\tilde{\sigma}_e^2} - \frac{\tilde{i}^2}{2\tilde{\sigma}_i^2} \right]. \quad (3)$$

We will also be using the dimensionless surface number density of guiding centers $N(H)$ to characterize the planetesimal spatial distribution.

Although we focus on a single embryo, for many applications we can treat the embryo using a continuous form of the evolution equations. For example, we may assume that the discrete surface number density of the embryo is given by

$$N_{em}(H) = \frac{1}{2\pi} \delta(m - M_e) \delta(H). \quad (4)$$

Since planetesimal-planetesimal interactions are not important here it will be enough to consider a single-mass planetesimal population.

The three-body interaction in the Hill approximation preserves a certain combination of relative orbital elements of interacting bodies called the Jacobi constant (Goldreich & Tremaine 1980; Hénon & Petit 1986):

$$J = \tilde{e}^2 + \tilde{i}^2 - \frac{3}{4} H^2 + 2\phi_e, \quad (5)$$

where ϕ_e is the gravitational potential of the embryo, which can be neglected far from the embryo. For embryo-planetesimal scattering one can introduce the concept of integrated Jacobi constant of the whole planetesimal population:

$$J^{tot} = \int_{-\infty}^{\infty} \left[2N(H)\tilde{\sigma}_e^2 + 2N(H)\tilde{\sigma}_i^2 - \frac{3}{4} N(H)H^2 \right] dH. \quad (6)$$

This quantity should be conserved because (1) each individual planetesimal scattering off the embryo conserves the Jacobi constant of the relative motion, and (2) embryo's random motion is negligible, which means that relative eccentricity, inclination, and difference in semimajor axes are determined by planetesimal orbital parameters only. We will use the conservation of this quantity and of the total number of planetesimals (we neglect their coagulation at this point)

$$N^{tot} = \int_{-\infty}^{\infty} N(H) dH. \quad (7)$$

as checks of our evolution equations.

The orbit integrations that we use are performed by solving Hill equations numerically. We have integrated the evolution of the system [equations of osculating orbital elements evolution (11) of Paper II] using fourth order Runge-Kutta integrator (Press *et al.* 1988). Unlike similar

calculations of Tanaka & Ida (1996, 1997) our orbit integrations do not employ additional analytical simplifications to avoid possible biases. In a typical integration the Jacobi constant is conserved with fractional accuracy $10^{-8} - 10^{-12}$. The results of these orbit integrations and their comparisons with theoretical predictions will be presented in the following sections.

We devote §2 to studying the shear-dominated case and §3 to exploring the dispersion-dominated case. The velocity regime intermediate between them is addressed in Appendix B. We discuss some general features of the embryo-planetesimal interaction in §5. Some auxiliary results are presented in appendices: Appendix A contains the derivation of the probability distribution of scattered semi-major axes in the dispersion-dominated regime, while in Appendix C we calculate the embryo’s accretion rate in different velocity regimes.

2. Scattering by the embryo in the shear-dominated regime.

We consider first the embryo-planetesimal interaction in the shear-dominated regime. In Paper II we have derived a master equation (30) for the evolution of the planetesimal distribution function. We will use this general equation and equation (33) of Paper II as a basis for our further developments. The conditions for the shear-dominated regime to be realized are

$$\tilde{\sigma}_e^2 \ll 1, \quad \tilde{\sigma}_i^2 \ll 1. \quad (8)$$

Some important simplifications can then be made.

First, scattering in this regime is deterministic in the sense that the outcome of an interaction between two particles depends only on their difference in semimajor axes before the collision H_0 and not on their relative random motion (which is naturally absent in this case). This means that the change of the reduced semimajor axis difference $\Delta\tilde{h}_{sc}$ ¹ is a single-valued function of only H_0 in this regime.

Second, inclination is hardly excited at all in the course of an encounter. A considerable change of inclination requires a substantial force acting in the vertical direction. However, the dynamically cold disk is very thin and it is easy to see that the gravitational force between the interacting particles is directed almost horizontally. Thus, noticeable inclination growth can occur only for particles experiencing very close encounters. From qualitative considerations one would expect that change of the inclination vector $\tilde{\mathbf{i}}$ (see Petit & Hénon 1986; Ida 1990; Paper II) is given by

$$\Delta(\tilde{\mathbf{i}}_{sc})^2 = \tilde{\mathbf{i}}_0^2 g_1(H_0) \ll 1, \quad (9)$$

where $\tilde{\mathbf{i}}_0$ is the initial value of the reduced vector inclination and $g_1(H_0) \sim 1$ is some function which can be easily computed numerically. For our purposes we neglect the inclination growth due to the

¹We use this notation instead of ΔH_{sc} to parallel the discussion of Paper II.

gravitational stirring in the shear-dominated regime completely and set $\Delta\tilde{\mathbf{i}}_{sc} = 0$. We will however keep the terms describing the transport of vertical energy in the disk (see below).

The absence of heating in the vertical direction naturally leads to another simplification. Since we can neglect the change of inclination in the encounter the change of eccentricity becomes directly related to the change of semimajor axis difference due to the conservation of Jacobi constant (5). Then we can write that the change of the vector eccentricity $\tilde{\mathbf{e}}$ is

$$\Delta(\tilde{\mathbf{e}}_{sc})^2 = \frac{3}{4}\Delta(\tilde{h}_{sc}^2) = \frac{3}{4}\left[(\Delta\tilde{h}_{sc})^2 + 2H_0\Delta\tilde{h}_{sc}\right]. \quad (10)$$

Note that $\Delta(\tilde{\mathbf{e}}_{sc})^2 \sim 1$ if $H_0 \sim 1$. It can also be easily shown that

$$\tilde{\mathbf{e}} \cdot \Delta\tilde{\mathbf{e}}_{sc} \sim \tilde{\mathbf{e}}^2 \ll 1, \quad \tilde{\mathbf{i}} \cdot \Delta\tilde{\mathbf{i}}_{sc} \sim \tilde{\mathbf{i}}^2 \ll 1 \quad (11)$$

in the shear-dominated regime; the corresponding scattering coefficients in evolution equations will therefore be neglected in this paper.

Thus, the probability \tilde{P}_r of scattering from $H_0, \tilde{\mathbf{e}}_0, \tilde{\mathbf{i}}_0$ to $H, \tilde{\mathbf{e}}, \tilde{\mathbf{i}}$ can be written in the shear-dominated regime as

$$\tilde{P}_r = \delta[\Delta H - \Delta\tilde{h}_{sc}(H_0)] \delta[\Delta\tilde{\mathbf{e}} - \Delta\tilde{\mathbf{e}}_{sc}(H_0)] \delta(\Delta\tilde{\mathbf{i}}), \quad (12)$$

where δ denotes the Dirac delta function.

The computational challenge of the shear-dominated regime is that strong scattering is possible for $H_0 \sim 1$, i.e. ΔH in the course of an encounter can be quite substantial. Thus we cannot use the Fokker-Planck formalism for the shear-dominated scattering and one has to deal with the different moments of the master evolution equation (30) of Paper II in their general form. However, this does not pose an insurmountable problem because the probability distribution function of the shear-dominated scattering is a single-variable function only. An analytical fit to this function was calculated by Petit & Hénon (1986, 1987b) using results of numerical orbit integrations. This fit automatically takes horseshoe motion into account so that we do not have to worry about the complications associated with this type of orbit in the shear-dominated regime: one can see from the expression for $\Delta\tilde{h}_{sc}(H_0)$ (Petit & Hénon 1987b) that $\Delta\tilde{h}_{sc}(H_0) \rightarrow -2H_0$ in the shear-dominated regime as $H_0 \rightarrow 0$.

Using the deterministic form of \tilde{P}_r [substituting expression (12) into equation (30) of Paper II] and the embryo's surface density in the form (4) we can take different moments of $\tilde{\mathbf{e}}^2$ and $\tilde{\mathbf{i}}^2$. As a result we find the following set of equations describing the evolution of the planetesimal population due to the scattering by the embryo in the shear-dominated regime:

$$\begin{aligned} \frac{\partial N(H)}{\partial t} &= -\frac{|A|\mu_e^{1/3}}{\pi} \left[N(H)|H| - \int_{-\infty}^{\infty} \tilde{P}(H_0, H) N(H_0) |H_0| dH_0 \right], \\ \frac{\partial}{\partial t} [2N(H)\tilde{\sigma}_e^2(H)] &= -\frac{|A|\mu_e^{1/3}}{\pi} \left[2N(H)\tilde{\sigma}_e^2(H)|H| \right. \end{aligned} \quad (13)$$

$$- \int_{-\infty}^{\infty} \tilde{P}(H_0, H) N(H_0) (2\tilde{\sigma}_e^2(H_0) + \Delta(\tilde{\mathbf{e}}_{sc})^2(H_0)) |H_0| dH_0 \Big], \quad (14)$$

$$\begin{aligned} \frac{\partial}{\partial t} [2N(H)\tilde{\sigma}_i^2(H)] &= -\frac{|A|\mu_e^{1/3}}{\pi} \\ &\times \left[2N(H)\tilde{\sigma}_i^2(H)|H| - \int_{-\infty}^{\infty} \tilde{P}(H_0, H) 2N(H_0)\tilde{\sigma}_i^2(H_0)|H_0| dH_0 \right], \end{aligned} \quad (15)$$

with $\mu_e = (M_e/M_c)^{1/3}$. Here A is the Oort's constant characterizing the differential rotation of the disk (Binney & Tremaine 1987), $A = -(3/4)\Omega$ in a Keplerian disk ($\Omega = \sqrt{GM_c/a_e^3}$ is the disk rotation frequency), H_0 is an integration variable having the meaning of the initial difference of the semimajor axes of interacting bodies, $\Delta(\tilde{\mathbf{e}}_{sc})^2$ is defined in equation (10), and

$$\tilde{P}(H_0, H) = \delta \left[H - H_0 - \Delta\tilde{h}_{sc}(H_0) \right]. \quad (16)$$

Terms in the r.h.s. of equation (15) are $\sim \tilde{\sigma}_i^2 \ll 1$, i.e. are of the same order as $\Delta(\tilde{\mathbf{i}}_{sc})^2$ which we have agreed to neglect. This inconsistency stems from the fact that we want our evolution equations to preserve the integrated Jacobi constant (6). For this reason we keep the terms in the r.h.s. of (15) (which are essentially the transport terms) but neglect terms like $\Delta(\tilde{\mathbf{i}}_{sc})^2$ if $\Delta(\tilde{\mathbf{e}}_{sc})^2$ is assumed to be given by (10). Then $\partial J^{tot}/\partial t = 0$ which can be verified using equations (10) and (13)-(15). Also, one can easily check that equation (13) conserves the total number of planetesimals in the disk.

One technical issue merits mentioning at this point. In the shear-dominated regime the semi-major axis difference after the encounter H is a single-valued function of H_0 . However, the inverse function $H_0(H)$ is multivalued (Petit & Hénon 1987b). For this reason integrals of some quantity $F(H_0)$ [e.g. $F = N(H_0)|H_0|$] over $\tilde{P}(H_0, H)dH_0$ in (13)-(15) result in

$$\int_{-\infty}^{\infty} \tilde{P}(H_0, H) F(H_0) dH_0 = \sum_k F(H_{0k}) \left[1 + \frac{\partial \Delta\tilde{h}_{sc}}{\partial H_0} \right]^{-1}, \quad (17)$$

where H_{0k} is the k -th root of the equation²

$$H = H_0 + \Delta\tilde{h}_{sc}(H_0). \quad (18)$$

The system (13)-(15) forms a closed set of equations needed to describe the disk evolution caused by embryo-planetesimal scattering in the shear-dominated regime. Equation (13) has already been derived by a different method in Paper I, and now we have extended that analysis by taking random velocity evolution of the disk into account. Following Paper I we will be using $\Delta\tilde{h}_{sc}(H_0)$ in the analytical form suggested by Petit & Hénon (1987b; see also Appendix B of Paper I).

²This form arises because of the integration rule of the Dirac δ -function: $\int_{-\infty}^{\infty} p(x)\delta[q(x)] = \sum_j p(x_j)/q'(x_j)$, where x_j is the j -th root of equation $q(x) = 0$.

3. Scattering by the embryo in the dispersion-dominated regime

When the embryo-planetesimal scattering is in the dispersion-dominated regime the same simplifications as in the case of planetesimal-planetesimal scattering can be made: scattering is weak and this warrants the use of both the two-body approximation and the Fokker-Planck expansion. In this regime we can use many of the results obtained in Paper II. There are however some additional complications; one of them is related to the aforementioned existence of horseshoe orbits. To discuss this issue we need to know which conditions should be fulfilled for horseshoe motion to take place in the dispersion-dominated velocity regime.

3.1. Horseshoe orbits.

Horseshoe motion arises when the separation of the semimajor axes of interacting bodies is small. In this case their relative motion due to the shear in the disk is very slow; for this reason even the weak gravitational force between the bodies at large azimuthal distance can lead to a considerable change of their angular momenta over a long time interval; the relative motion of particles reverses, they turn around and move on almost closed trajectories until the next conjunction (see Figure 1a). In the Solar System the best example of such motion is given by Saturnian satellites Janus & Epimetheus (Murray & Dermott 1999).

In contrast, planetesimals on passing orbits pass each other after the interaction, usually without reversing their motion (see Figure 1b). In the shear-dominated regime these orbits typically have initial separations of semimajor axes larger than the Hill radius. However in dispersion-dominated encounters the question of the spatial separation of horseshoe and passing orbits becomes more subtle.

Namouni (1999) has considered dispersion-dominated scattering in the planar case ($\tilde{i} = 0$) and suggested that for a given relative eccentricity $\tilde{e} \gg 1$ the boundary of the horseshoe region is located at $H = \tilde{h}_{hs} \sim \tilde{e}^{-1/2}$ [see also Ida & Nakazawa (1989)]. This means that the more “energetic” the planetesimals are, the smaller their semimajor axis separation has to be for horseshoe motion to appear. This tendency is illustrated in Figure 1: orbits with the same value of $H = 0.7$ exhibit different behavior depending on their random velocities — in the shear-dominated regime ($\tilde{e} = \tilde{i} = 0$) horseshoe motion takes place while in the dispersion-dominated ($\tilde{e} = \tilde{i} = 5$) the orbit is passing; however if one decreases H this orbit also becomes horseshoe (which is shown by a trajectory with $H = 0.3, \tilde{e} = \tilde{i} = 5$ in Figure 1a). It is easy to understand the reason for this dependence on the planetesimal random velocity: the higher the eccentricity the more time the approaching planetesimal spends far from the scatterer because it moves on a very large epicycle. As a result the mutual force is weak, the angular momentum exchange is small, and the planetesimal passes the scatterer instead of turning around. In other words, the higher \tilde{e} the less noticeable the presence of the scatterer is for the incoming planetesimal.

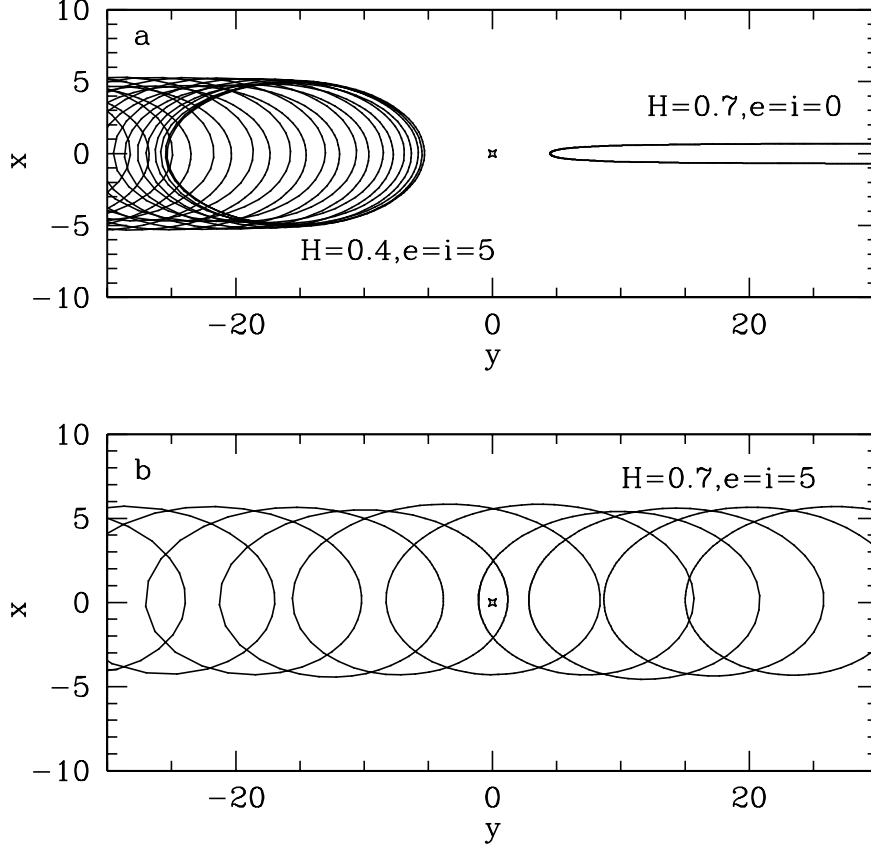


Fig. 1.— Representative trajectories of bodies on horseshoe (a) and passing (b) orbits for different values of initial orbital elements. The scattering body is at the origin and the coordinates are in units of the Hill radius.

In the nonplanar case, on the basis of similar arguments, we suggest that the horseshoe boundary condition in the high-velocity regime should be replaced with

$$\tilde{h}_{hs} = \left(\frac{k}{\tilde{e}^2 + \tilde{i}^2} \right)^{1/4}. \quad (19)$$

To check this prediction and fix the proportionality constant k , we have performed a set of orbit integrations in both the shear- and dispersion-dominated regimes. We have separated the outcomes of encounters into horseshoe orbits (when H was changing sign as a result of an encounter) and passing ones (when the sign of H remained unchanged). The results are presented in Figure 2. One can see a rather clean separation between the horseshoe orbits (red dots) and passing ones (blue dots). There are some red dots which appear in the region mostly occupied by the passing orbits, but they originate from large-angle scattering during close encounters and are not librating orbits as normal horseshoes are.

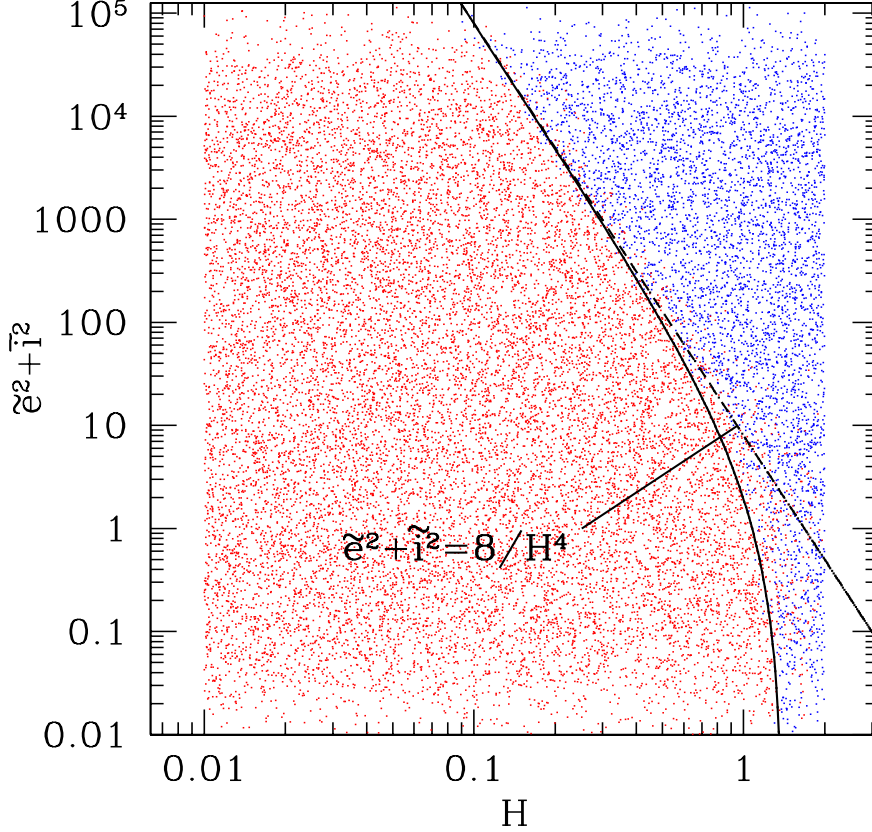


Fig. 2.— Horseshoe and passing orbits as a function of the orbital parameters H and $\tilde{e}^2 + \tilde{i}^2$. Red ones correspond to horseshoe orbits, blue ones to passing orbits. The solid line is the analytical expression (20) for the boundary. The dashed line shows the power law asymptote of this relation in the strongly dispersion-dominated regime.

The separation condition (19) fits the boundary between the two types of orbits very well when $\tilde{e}^2 + \tilde{i}^2 \gg 1$ if we take $k \simeq 8$ (dashed curve in Figure 2). However, as we move away from the strongly dispersion-dominated regime some deviations from (19) appear. This is not surprising because small \tilde{e} and \tilde{i} correspond to the shear-dominated regime, and then the horseshoe region has a well-defined boundary at $\tilde{h}_{hs} \sim 1$. We have found that the shape of the horseshoe-passing boundary can be fit rather accurately by the following condition

$$\tilde{e}^2 + \tilde{i}^2 = R_{hs}^2(\tilde{h}_{hs}) = k \left(\frac{1}{\tilde{h}_{hs}^2} - \frac{1}{b^2} \right)^2, \quad \tilde{h}_{hs} < b, \quad k \simeq 8, \quad b \simeq 1.4 \quad (20)$$

which is shown by the solid curve on Figure 2³.

³Our value of b would predict \tilde{h}_{hs} in the shear-dominated regime slightly different from that suggested by Petit & Hénon (1987b): $\simeq 1.4$ instead of $\simeq 1.2$. However, such a small difference is unlikely to be important for our purposes.

Using distribution function of eccentricities and inclinations (3) we can calculate the fraction of passing orbits ρ_{pass} :

$$\rho_{pass}(H) = \begin{cases} \exp\left[-\frac{R_{hs}^2(H)}{2\tilde{\sigma}_e^2}\right] + \frac{\tilde{\sigma}_i^2}{\tilde{\sigma}_i^2 - \tilde{\sigma}_e^2} \left\{ \exp\left[-\frac{R_{hs}^2(H)}{2\tilde{\sigma}_i^2}\right] - \exp\left[-\frac{R_{hs}^2(H)}{2\tilde{\sigma}_e^2}\right] \right\}, & H < b, \\ 1, & H > b. \end{cases} \quad (21)$$

One can see that $\rho_{pass}(H)$ changes rapidly from 0 to 1 between the regions of horseshoe and passing orbits (this is caused by the exponential dependence of ρ_{pass} on R_{hs} and the strong power law dependence of R_{hs} on H). This allows us to neglect the transition region in the dispersion-dominated regime and assume these different types of orbits to occupy different regions of the physical space. Thus we take passing orbits to be restricted to the region $|H| > \tilde{h}_{hs}$ where \tilde{h}_{hs} is defined such that

$$\rho_{pass}(\tilde{h}_{hs}) = 1/2, \quad (22)$$

and horseshoe orbits to satisfy $|H| < \tilde{h}_{hs}$. Using these conditions we can now consider passing orbits separately from the horseshoe ones.

3.2. Scattering on horseshoe orbits.

The relative motion of interacting planetesimals in the horseshoe regime can be split into the slow shear motion of the guiding centers and the fast epicyclic motion. When such a separation is legitimate some quantities associated with the fast motion called adiabatic invariants should be conserved (Landau & Lifshitz 1989). It was shown by Hénon & Petit (1986) and Hasegawa & Nakazawa (1990) that the absolute value of the relative semimajor axis difference, relative eccentricity and relative inclination are all separately conserved quantities in the course of a horseshoe encounter, and that they are the adiabatic invariants of this type of motion. Thus the quantities $H_0, \tilde{\mathbf{e}}_0, \tilde{\mathbf{i}}_0$ before the encounter are related to their values after, $H, \tilde{\mathbf{e}}, \tilde{\mathbf{i}}$, as

$$H = -H_0, \quad \tilde{\mathbf{e}} = \tilde{\mathbf{e}}_0, \quad \tilde{\mathbf{i}} = \tilde{\mathbf{i}}_0 \quad (23)$$

It follows from this conservation of adiabatic invariants that the effect of the embryo-planetesimal encounters in the horseshoe region is to exchange planetesimals at symmetric orbits (H and $-H$). Interacting bodies just librate between successive close approaches when they reverse the direction of their motion.

Because the embryo is much more massive than the planetesimals and its \tilde{e} and \tilde{i} are zero, the relative motion in the embryo-planetesimal system is equivalent to the motion of planetesimals. The scattering probability for the horseshoe motion \tilde{P}_{hs} looks like $\tilde{P}_{hs} = \delta(\Delta H + 2H_0)\delta(\Delta \tilde{\mathbf{e}})\delta(\Delta \tilde{\mathbf{i}})$. Using this result we can write down the evolution equation of some quantity F by analogy with equations (13)-(15) in a very simple form:

$$\frac{\partial F(H)}{\partial t} = \frac{|A|\mu_e^{1/3}}{\pi} |H| [F(-H) - F(H)]. \quad (24)$$

In our case F can be the planetesimal surface density N , horizontal epicyclic energy $N\tilde{\sigma}_e^2$ or vertical epicyclic energy $N\tilde{\sigma}_i^2$.

3.3. Scattering on passing orbits.

To describe the embryo-planetesimal interaction on passing orbits in the dispersion-dominated regime we will use the results for the scattering in this regime derived in Paper II, namely equations (49)-(51) and (52)-(55). We substitute embryo's surface number density in the form (4) for the surface density of approaching bodies N_2 , assume that $m/M_e \rightarrow 0$ and that $\tilde{\sigma}_{e2} = \tilde{\sigma}_{i2} = 0$. As a result we obtain the following system

$$\frac{\partial N}{\partial t} = \frac{|A|\mu_e^{1/3}}{\pi} \left[-\frac{\partial}{\partial H} \left(|H| \langle \Delta \tilde{h} \rangle N \right) + \frac{1}{2} \frac{\partial^2}{\partial H^2} \left(|H| \langle (\Delta \tilde{h})^2 \rangle N \right) \right], \quad (25)$$

$$\begin{aligned} \frac{\partial}{\partial t} [2N(H)\tilde{\sigma}_e^2(H)] &= \frac{|A|\mu_e^{1/3}}{\pi} \\ &\times \left[|H| \langle \Delta(\tilde{\mathbf{e}}^2) \rangle N - \frac{\partial}{\partial H} \left(|H| \langle (\tilde{\mathbf{e}}^2 + 2\tilde{\mathbf{e}} \cdot \Delta \tilde{\mathbf{e}}) \Delta \tilde{h} \rangle N \right) + \frac{1}{2} \frac{\partial^2}{\partial H^2} \left(|H| \langle \tilde{\mathbf{e}}^2 (\Delta \tilde{h})^2 \rangle N \right) \right], \end{aligned} \quad (26)$$

and an equation for the inclination evolution analogous to (26). These formulae are only valid in the region of space restricted by the condition (22). Analytical expressions for the scattering coefficients $\langle \Delta \tilde{h} \rangle$, $\langle (\Delta \tilde{h})^2 \rangle$, $\langle \Delta(\tilde{\mathbf{e}}^2) \rangle$, $\langle (\tilde{\mathbf{e}}^2 + 2\tilde{\mathbf{e}} \cdot \Delta \tilde{\mathbf{e}}) \Delta \tilde{h} \rangle$, and $\langle \tilde{\mathbf{e}}^2 (\Delta \tilde{h})^2 \rangle$ can be found in Paper II. The proper boundary conditions for this system will be derived in §3.3.1.

At this point we should address a subtle issue which was not important for the planetesimal-planetesimal scattering but becomes nontrivial for the embryo-planetesimal interaction. It is related to the fact that planetesimals at different initial separations are driven past the embryo by the differential shear at different rates. Those which initially had $|H| \gg 1$ quickly approach the embryo, experience scattering, and quickly depart. On the approach and departure stages their orbital parameters do not have time to change except when they are close to the embryo. Thus, we can assume that values of $H, \tilde{\mathbf{e}}, \tilde{\mathbf{i}}$ far from the embryo are the same as at the point of closest approach if initially $|H| \gg 1$.

However, planetesimals which start their motion not far from the horseshoe orbits boundary are not moving very fast (because this boundary is located at $\tilde{h}_{hs} \leq R_H$). As a result, for these planetesimals the exchange of the angular momentum before and after the close encounter can be important, just as in the case of horseshoe orbits, where such an exchange essentially prevents close encounters from happening. Consequently, the asymptotic value of the separation H is not the same as its value at the close encounter. We must also ask whether the eccentricity and inclination are affected in a similar way. In this situation $\tilde{\mathbf{e}}$ and $\tilde{\mathbf{i}}$ are not perfectly conserved adiabatic invariants (frequencies of the two superposed motions are not very strongly different from each other) but we probably will not make a huge mistake by assuming that they still are conserved on the approach and departure stages. Thus, we can draw the following picture of scattering for these orbits: as

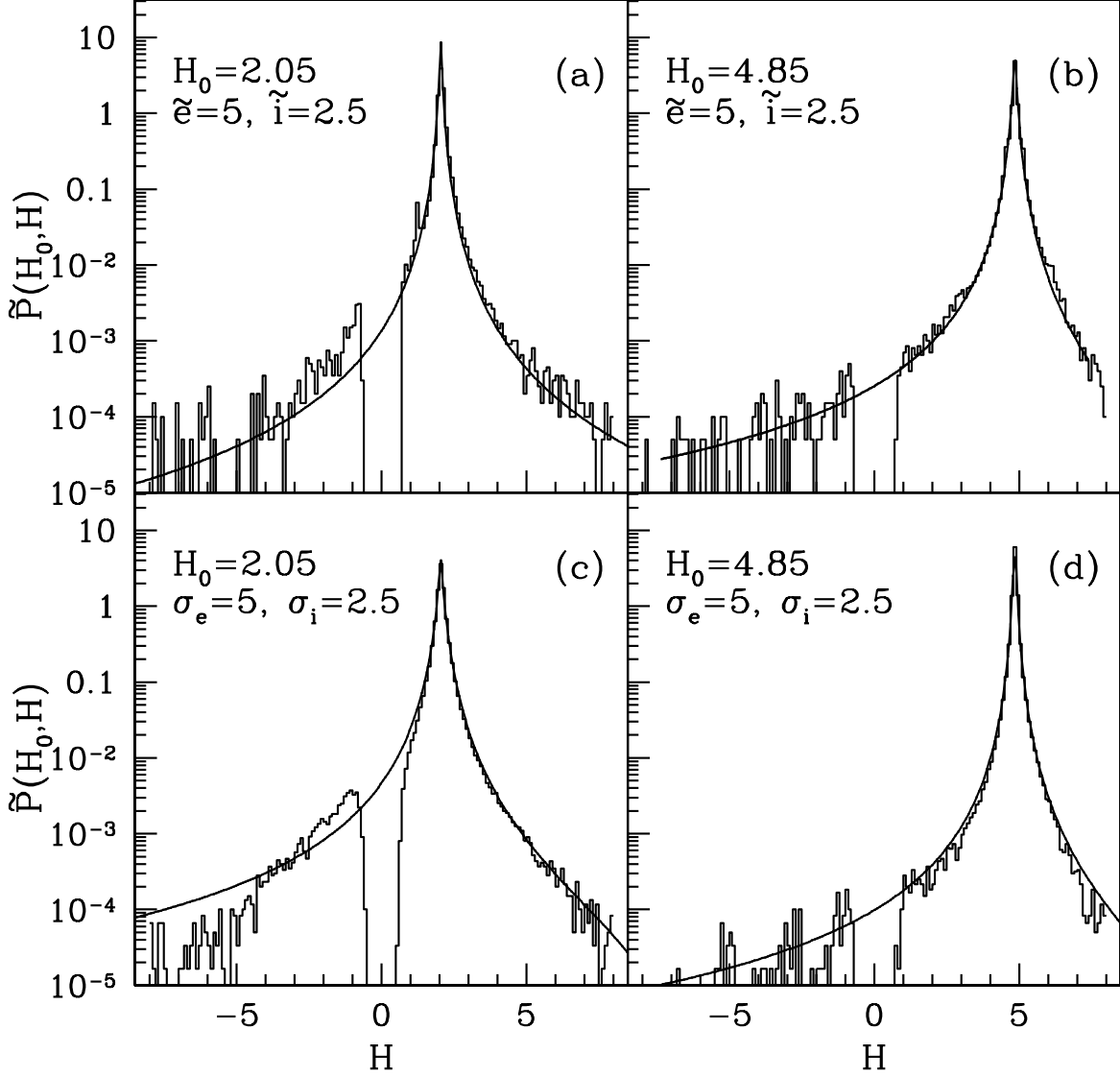


Fig. 3.— Scattering probability $\tilde{P}(H_0, H)$ as a function of the final orbital separation H for a fixed initial separation H_0 . The probability is calculated by binning the outcomes of orbit integrations (*histogram*) and also analytically in Appendix A (*solid line*). Panels (a,b) display $\tilde{P}(H_0, H)$ for fixed values of the initial eccentricity and inclination $\tilde{e} = \tilde{i} = 5$ and two values of the initial orbital separation, $H_0 = 2.05$ and 4.85 . Panels (c,d) display $\tilde{P}(H_0, H)$ for fixed values of the initial dispersions of eccentricity and inclination, $\tilde{\sigma}_e = \tilde{\sigma}_i = 5$. Note the absence of scattered orbits near $H = 0$ caused by the angular momentum exchange at large azimuthal distances (see text).

the planetesimal gets closer to the embryo the absolute value of H gets smaller as a result of the angular momentum exchange with the embryo, while the eccentricity and inclination are preserved (see Figure 4). At the point of closest approach, the planetesimal orbital parameters experience a quick variation as a result of close encounter with the embryo. After that, on the departure stage, the embryo slowly changes the angular momentum of the planetesimal such that $|H|$ increases.

These variations of H at constant \tilde{e} and \tilde{i} do not contradict the conservation of the Jacobi constant (5) because the gravitational potential due to the embryo changes in the course of planetesimal approach and departure as well. In fact, using the conservation of Jacobi constant we derive a prescription for the relation between the semimajor axis difference H far from the embryo and its value at the moment of the close encounter, H' . To do this we note that at the moment of the closest approach the distance between the embryo and planetesimal in units of the embryo's Hill radius is of order $\sqrt{\tilde{e}^2 + \tilde{i}^2}$. Then the conservation of the Jacobi constant (5) tells us that $H^2 - (H')^2 \sim (\tilde{e}^2 + \tilde{i}^2)^{-1/2}$. This empirical expression may be inaccurate if one applies it for $\tilde{e}, \tilde{i} \leq 1$. This can be remedied using the following approximate prescription

$$(H')^2 = H^2 - \frac{c}{\sqrt{\tilde{e}^2 + \tilde{i}^2 + d^2}}, \quad c \simeq 1.8, \quad d \simeq 2, \quad (27)$$

where the numerical values of constants c and d were fixed by comparison with orbit integrations. Whenever the planetesimal disk has a distribution of eccentricities and inclinations we replace \tilde{e} and \tilde{i} in (27) with $\tilde{\sigma}_e$ and $\tilde{\sigma}_i$. The relationship (27) is certainly not very accurate. However, this transformation is satisfactory for our purposes since the complete separation of horseshoe and passing orbits we are assuming is a rather crude approximation anyway.

To better understand the consequences and importance of this effect it is instructive to look at the distribution function of planetesimal scattering $\tilde{P}(H_0, H)$ in the dispersion-dominated regime [by definition $\tilde{P}(H_0, H)dH$ is the probability that a planetesimal initially at H_0 is scattered into the interval $(H, H + dH)$]. We calculate this function analytically in Appendix A and represent it in the following form:

$$\tilde{P}(H_0, H) = \frac{1}{2 \ln \Lambda} \frac{\langle (\Delta \tilde{h})^2 \rangle + \langle \Delta \tilde{h} \rangle \Delta H}{(|\Delta H| + d)^3}, \quad \Delta H = H - H_0, \quad (28)$$

where

$$d \approx \left[\frac{\langle (\Delta \tilde{h})^2 \rangle}{2 \ln \Lambda} \right]^{1/2}, \quad (29)$$

$\langle \Delta \tilde{h} \rangle$ and $\langle (\Delta \tilde{h})^2 \rangle$ are the scattering coefficients (see Paper II), and $\ln \Lambda$ is the usual Coulomb logarithm. To compute $\tilde{P}(H_0, H)$ accounting for the distribution of planetesimal eccentricities and inclinations one simply needs to use the values of $\langle \Delta \tilde{h} \rangle$ and $\langle (\Delta \tilde{h})^2 \rangle$ averaged over this distribution (they are given in §4 of Paper II for the case of Gaussian distribution of \tilde{e} and \tilde{i}).

One can also obtain this distribution function from numerical orbit integrations. To do this we perform Monte-Carlo simulations in two different ways: by fixing the absolute values of the

eccentricity and inclination of the planetesimals (only their epicyclic phases are chosen randomly), and by picking their orbital elements from the distribution (3) with fixed dispersions. In both cases the initial difference of semimajor axes H_0 is the same for each simulation. In Figure 3a,b we plot $\tilde{P}(H_0, H)$ for fixed $\tilde{e} = 2\tilde{i} = 5$ and in Figure 3c,d we do this for fixed $\tilde{\sigma}_e = 2\tilde{\sigma}_i = 5$. The analytical distribution given by (28) is also plotted for each case. One can see that it generally agrees very well with the numerical results. The large variations of $\tilde{P}(H_0, H)$ in the outer wings of the simulated distributions are caused by statistical noise. When $|H - H_0| \leq 1$ the agreement between theory and simulations is quite remarkable even for the distributions averaged over \tilde{e}, \tilde{i} (Figure 3c,d).

However, one can also immediately notice one important feature of the simulated $\tilde{P}(H_0, H)$: there are no orbits scattered in a region with a width $\sim R_H$ around the embryo’s location, and this is in contrast with the analytical result (28) which exhibits no such feature. A similar “gap” in the distribution of scattered orbits can also be noticed in the numerical calculations performed by Greenzweig & Lissauer (1990) and Ohtsuki & Tanaka (2002).

From our previous discussion the reason for the appearance of this gap becomes quite apparent. It is the gravitational interaction of the particles on passing orbits located close to the horseshoe region with the embryo which drives them away from its orbit, corresponding to $H = 0$. If we were to take the same probability distributions not far away from the embryo in the azimuthal direction but immediately after the scattering (within $\sim R_H$ from the embryo along the azimuthal direction) we would not find such a “gap”. However, as the differential shear slowly increases the azimuthal separation of the interacting bodies their mutual angular momentum exchange leads to a gradual increase of $|H|$ similar to that happening on the horseshoe orbits. As a result, a conspicuous “gap” appears in $\tilde{P}(H_0, H)$ near $H = 0$. This process is illustrated in Figure 4.

This effect has important consequences for the calculation of scattering on passing orbits with radial separations $\sim R_H$ (or $|H| \sim 1$). The difference between H far from the embryo (which we take as one of the planetesimal coordinates) and its value at the moment of the close encounter introduces changes into the computation of scattering coefficients. Indeed, if before and after the encounter the values of planetesimal semimajor axis are H_0 and H , and at the point of closest approach it has the value of H' , we can write that (see Figure 4)

$$H'(H_0) + \Delta\tilde{h}'[H'(H_0)] = H'(H_0 + \Delta\tilde{h}), \quad (30)$$

where $\Delta\tilde{h}'$ and $\Delta\tilde{h}$ are changes of H' and H correspondingly. Our calculation of scattering coefficients in §4 of Paper II gives us only the value of $\Delta\tilde{h}'$ (change of the planetesimal semimajor axis at the closest approach). Here however we are interested in $\Delta\tilde{h} = H - H_0$. To relate them we assume that both changes are small which is always a good approximation in the dispersion-dominated regime. Then, expanding the r.h.s. of (30) up to the second order in $\Delta\tilde{h}$ we find that

$$\begin{aligned} \Delta\tilde{h}(H_0) &= \left(\frac{\partial H'}{\partial H_0}\right)^{-1} \Delta\tilde{h}' - \frac{1}{2} \frac{\partial^2 H'}{\partial H_0^2} \left(\frac{\partial H'}{\partial H_0}\right)^{-3} (\Delta\tilde{h}')^2 + O((\Delta\tilde{h}')^3), \\ (\Delta\tilde{h}(H_0))^2 &= \left(\frac{\partial H'}{\partial H_0}\right)^{-2} (\Delta\tilde{h}')^2 + O((\Delta\tilde{h}')^3). \end{aligned} \quad (31)$$

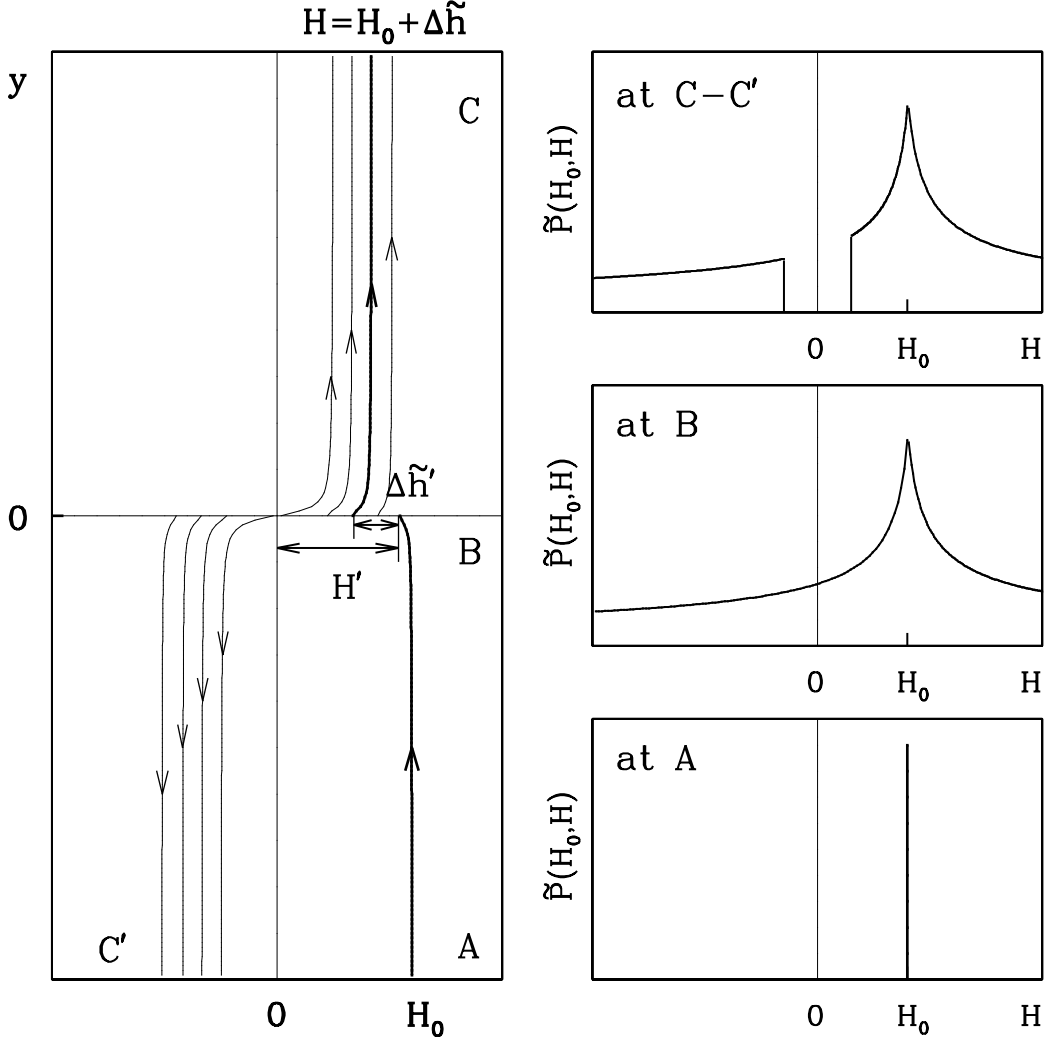


Fig. 4.— Schematic illustration of planetesimal scattering on passing orbits near the horseshoe-passing orbits boundary. The thick solid line in the left panel represents the track of the guiding center of some planetesimal initially located at H_0 . As a result of angular momentum exchange with the embryo its semimajor axis shifts to H' prior to scattering; then in the course of a close encounter it is changed by $\Delta\tilde{h}'$. Subsequent interaction with the embryo on the departure stage increases the semimajor axis from $H' + \Delta\tilde{h}'$ to H . Note that $\Delta\tilde{h} = H - H_0$ is not equal to $\Delta\tilde{h}'$. Thin solid lines show the trajectories of planetesimals with the same H_0 but different epicyclic phases. The panels on the right illustrate the origin of the gap in the probability distribution of scattering by plotting snapshots of the semimajor axes distribution of planetesimals $\tilde{P}(H_0, H)$ initially (where it has δ -function form, at point A), immediately after the encounter (at point B), and long after (points C and C' coincide in the closed box).

At the same time our assumption of approximate adiabatic conservation of $\tilde{\mathbf{e}}$ and $\tilde{\mathbf{i}}$ implies that the changes of these quantities evaluated far from the embryo are the same as they are in the course of an encounter near the embryo. It also means that in calculating scattering coefficients we should use the values of eccentricity and inclination characterizing the planetesimal orbit far from the embryo.

The relationships represented by equations (31) are utilized when we calculate scattering coefficients in equations (25)-(26).

3.3.1. Boundary conditions for the scattering on passing orbits.

The simplest way to derive the boundary conditions for equations (25)-(26) is to consider the Fokker-Planck equation for the evolution of the distribution function of planetesimals $f(\mathbf{\Gamma})$ caused by embryo-planetesimal encounters. Here $\mathbf{\Gamma}$ is a set of orbital elements characterizing the planetesimal orbital state: $\Gamma_1 = H, (\Gamma_2, \Gamma_3) = \tilde{\mathbf{e}}$ (vector eccentricity) and $(\Gamma_4, \Gamma_5) = \tilde{\mathbf{i}}$ (vector inclination). Following conventional wisdom (Lifshitz & Pitaevskii 1981; Binney & Tremaine 1987) we can write the evolution equation of f caused by weak encounters:

$$\frac{\partial f}{\partial t} = -2|A| \left[\sum_{i=1}^5 \frac{\partial}{\partial \Gamma_i} (f|H|\langle \Delta \Gamma_i \rangle) + \frac{1}{2} \sum_{i=1}^5 \frac{\partial^2}{\partial \Gamma_i \partial \Gamma_j} (f|H|\langle \Delta \Gamma_i \Delta \Gamma_j \rangle) \right] = -\frac{\partial F_i}{\partial \Gamma_i}, \quad (32)$$

where the flux in the i -th direction is given by

$$F_i = 2|A| \left[f|H|\langle \Delta \Gamma_i \rangle - \frac{1}{2} \sum_{i=1}^5 \frac{\partial}{\partial \Gamma_j} (f|H|\langle \Delta \Gamma_i \Delta \Gamma_j \rangle) \right]. \quad (33)$$

Averaging of quantities like $\langle \Delta \Gamma_i \rangle$ is performed here only over the possible outcomes of scattering and not over $d\tilde{\mathbf{e}}d\tilde{\mathbf{i}}$. The factor $2|A||H|$ takes care of the linear shear velocity in the planetesimal disk (changes of various quantities caused by the scattering are assumed to be per encounter and not per unit of time). Note that we could have obtained equations (25)-(26) directly from (32).

Particles on passing orbits do not penetrate into the region of horseshoe orbits (as a result of our presumed complete separation of these two types of orbits). Thus the component of the flux F_H must vanish at the boundaries $H = \tilde{h}_{hs}$ and $H = -\tilde{h}_{hs}$:

$$\begin{aligned} & f|H|\langle \Delta H \rangle - \frac{1}{2} \frac{\partial}{\partial (\tilde{\mathbf{e}}^2)} [f|H|\langle \Delta H \Delta (\tilde{\mathbf{e}}^2) \rangle] \\ & - \frac{1}{2} \frac{\partial}{\partial (\tilde{\mathbf{i}}^2)} [f|H|\langle \Delta H \Delta (\tilde{\mathbf{i}}^2) \rangle] - \frac{1}{2} \frac{\partial}{\partial H} [f|H|\langle (\Delta H)^2 \rangle] = 0 \quad \text{at } H = \pm \tilde{h}_{hs}. \end{aligned} \quad (34)$$

Our next step is to multiply condition (34) by $d(\tilde{\mathbf{e}}^2)d(\tilde{\mathbf{i}}^2)$, $\tilde{\mathbf{e}}^2 d(\tilde{\mathbf{e}}^2)d(\tilde{\mathbf{i}}^2)$ and $\tilde{\mathbf{i}}^2 d(\tilde{\mathbf{e}}^2)d(\tilde{\mathbf{i}}^2)$ and integrate it over $\tilde{\mathbf{e}}^2$ - $\tilde{\mathbf{i}}^2$ space. We obtain as a result (integrating by parts where needed) that

$$N|H|\langle \Delta \tilde{h} \rangle - \frac{1}{2} \frac{\partial}{\partial H} [N|H|\langle (\Delta \tilde{h})^2 \rangle] = 0, \quad (35)$$

$$N|H|\langle\tilde{\mathbf{e}}^2\Delta\tilde{h}\rangle - \frac{1}{2}\frac{\partial}{\partial H}\left[N|H|\langle\tilde{\mathbf{e}}^2(\Delta\tilde{h})^2\rangle\right] + \frac{1}{2}N|H|\langle\Delta(\mathbf{e}^2)\Delta\tilde{h}\rangle = 0, \quad (36)$$

$$N|H|\langle\tilde{\mathbf{i}}^2\Delta\tilde{h}\rangle - \frac{1}{2}\frac{\partial}{\partial H}\left[N|H|\langle\tilde{\mathbf{i}}^2(\Delta\tilde{h})^2\rangle\right] + \frac{1}{2}N|H|\langle\Delta(\tilde{\mathbf{i}}^2)\Delta\tilde{h}\rangle = 0 \quad \text{at } H = \pm\tilde{h}_{hs}, \quad (37)$$

where now $\langle\ldots\rangle$ means integration not only over the probability distribution of scattering but also over the $\tilde{\mathbf{e}}^2$ - $\tilde{\mathbf{i}}^2$ space (and we use the more familiar notation $\langle\Delta\tilde{h}\rangle$ instead of $\langle\Delta H\rangle$, etc.). In getting these results we have taken into account that all scattering coefficients vanish at the boundaries of the velocity space (which are at infinity).

As we discussed in Paper II terms like $\langle(\Delta\tilde{\mathbf{e}})^2\Delta\tilde{h}\rangle$ are third order in perturbations and can be neglected. Thus we can approximate $\langle\Delta(\tilde{\mathbf{e}}^2)\Delta\tilde{h}\rangle$ with $2\langle(\tilde{\mathbf{e}} \cdot \Delta\tilde{\mathbf{e}})\Delta\tilde{h}\rangle$. As a result we find that

$$N|H|\langle\Delta\tilde{h}\rangle - \frac{1}{2}\frac{\partial}{\partial H}\left[N|H|\langle(\Delta\tilde{h})^2\rangle\right] = 0, \quad (38)$$

$$N|H|\langle(\tilde{\mathbf{e}}^2 + \tilde{\mathbf{e}} \cdot \Delta\tilde{\mathbf{e}})\Delta\tilde{h}\rangle - \frac{1}{2}\frac{\partial}{\partial H}\left[N|H|\langle\tilde{\mathbf{e}}^2(\Delta\tilde{h})^2\rangle\right] = 0, \quad (39)$$

$$N|H|\langle(\tilde{\mathbf{i}}^2 + \tilde{\mathbf{i}} \cdot \Delta\tilde{\mathbf{i}})\Delta\tilde{h}\rangle - \frac{1}{2}\frac{\partial}{\partial H}\left[N|H|\langle\tilde{\mathbf{i}}^2(\Delta\tilde{h})^2\rangle\right] = 0 \quad \text{at } H = \pm\tilde{h}_{hs}. \quad (40)$$

Note the specific combination $\tilde{\mathbf{e}}^2 + \tilde{\mathbf{e}} \cdot \Delta\tilde{\mathbf{e}}$, not $\tilde{\mathbf{e}}^2 + 2\tilde{\mathbf{e}} \cdot \Delta\tilde{\mathbf{e}}$ as in equation (26) — this is important for the conservation of the Jacobi constant.

Do equations (25)-(26) conserve the integrated Jacobi constant (6) and the total number of planetesimals (7)? If we integrate (25) over dH (which would give us the total number of planetesimals in the region of interest), we find that condition (38) ensures the conservation of N^{tot} . The same is true for the integrated Jacobi constant: when we substitute equations (25)-(26) into the definition (6) we find (after some cumbersome but straightforward calculations) that conditions (38)-(40) guarantee the conservation of J^{tot} up to the second order in the perturbed quantities. Thus, expressions (38)-(40) provide a desired set of self-consistent boundary conditions for the equations (25)-(26).

3.3.2. Comparison with numerical orbit integrations.

To check our predictions about the behavior of the planetesimal disk properties derived in the previous sections we have performed a set of numerical simulations. We have integrated the orbits of test particles, starting at large azimuthal separation from the embryo, and observe the changes of their orbital parameters as they experience gravitational interactions with the planetary embryo. Initial orbital parameters are chosen randomly from the distribution of eccentricities and inclinations (3). The semimajor axes of particles are assumed to be uniformly distributed within some radial interval around the embryo. The width of this interval is large enough that boundary effects are not important. We typically calculate about 2×10^5 different orbits to reduce statistical noise. Each orbit experiences several hundred passages past the embryo during which its orbital elements change. Between the conjunctions we randomize the epicyclic phases of the

planetesimals to mimic the effect of planetesimal-planetesimal interaction which is assumed to destroy any resonances in the system (the hypothesis of molecular chaos). However the absolute values of eccentricity and inclination are not affected by this procedure. In the course of the integration embryo is assumed to be immobile.

The number of consecutive passages is dictated by the condition that the system evolves for at least one dynamical time within region of phase space for which close encounters can occur $|H| \leq \tilde{\sigma}_e$. In the shear-dominated regime this corresponds to a single passage at radial separation $\sim R_H$ (i.e. dynamical time $t_{dyn} \sim t_{syn}$ — synodic period at $H = 1$) because scattering is strong in this case. At the same time equations (25)-(26) and analytical expressions for the scattering coefficients in Paper II show that in the dispersion-dominated regime the dynamical time $t_{dyn} \sim t_{syn} \tilde{\sigma}_e^5$ when $\tilde{\sigma}_e \sim \tilde{\sigma}_i$. This timescale can easily take several hundred orbital passages which require that one follow planetesimal orbital evolution for rather a long time.

In Appendix B we describe our treatment of the intermediate (between shear- and dispersion-dominated) velocity regime and make comparisons with the results of orbit integrations. Here we perform this procedure for the dispersion-dominated regime. In Figures 5 and 6 we display time sequences of profiles of horizontal and vertical velocity dispersions [panels (a,b) and (c,d) correspondingly], and dimensionless surface density normalized by its value at infinity [panels (e,f)]. We show both the results of orbit integrations (left row of panels) and our analytical predictions (right row of panels). Disk evolution in the region of the horseshoe orbits is described using equation (24). In the region of passing orbits [outside of the interval $(-\tilde{h}_{hs}, \tilde{h}_{hs})$, see §3.1] disk evolution is governed by partial differential evolution equations (25)-(26). We solve them using fully implicit scheme (Press *et al.* 1988) with the boundary conditions (38)-(40) imposed at $H = -\tilde{h}_{hs}$ and $H = \tilde{h}_{hs}$ and scattering coefficients computed analytically in Paper II. The conversion (27) is used throughout the calculation and the boundary of the horseshoe region is described by formula (22). For the factor Λ entering the Coulomb logarithm in the expressions for the scattering coefficients we use the following prescription⁴:

$$\Lambda = \tilde{\sigma}_i(2\tilde{\sigma}_e^2 + \tilde{\sigma}_i^2). \quad (41)$$

Constant coefficients in this formula are roughly fixed using comparison with orbit integrations (but our final results depend on them very weakly).

Figure 5 shows the disk evolution in the case when the initial planetesimal dispersions of eccentricity and inclination are both equal to 3. One can see an excellent qualitative agreement between the results of orbit integrations and analytical theory. All the features of the spatial distributions of disk quantities are well reproduced by the solutions of the analytical equations. There is also a reasonable degree of quantitative agreement between them although there are also some minor differences: the analytical equations predict somewhat faster evolution of $\tilde{\sigma}_i$ and a

⁴To avoid problems at $\tilde{\sigma}_e, \tilde{\sigma}_i \leq 1$ we use instead of $\ln \Lambda$ the more accurate expression $(1/2) \ln(1 + \Lambda^2)$ (see Binney & Tremaine 1987).

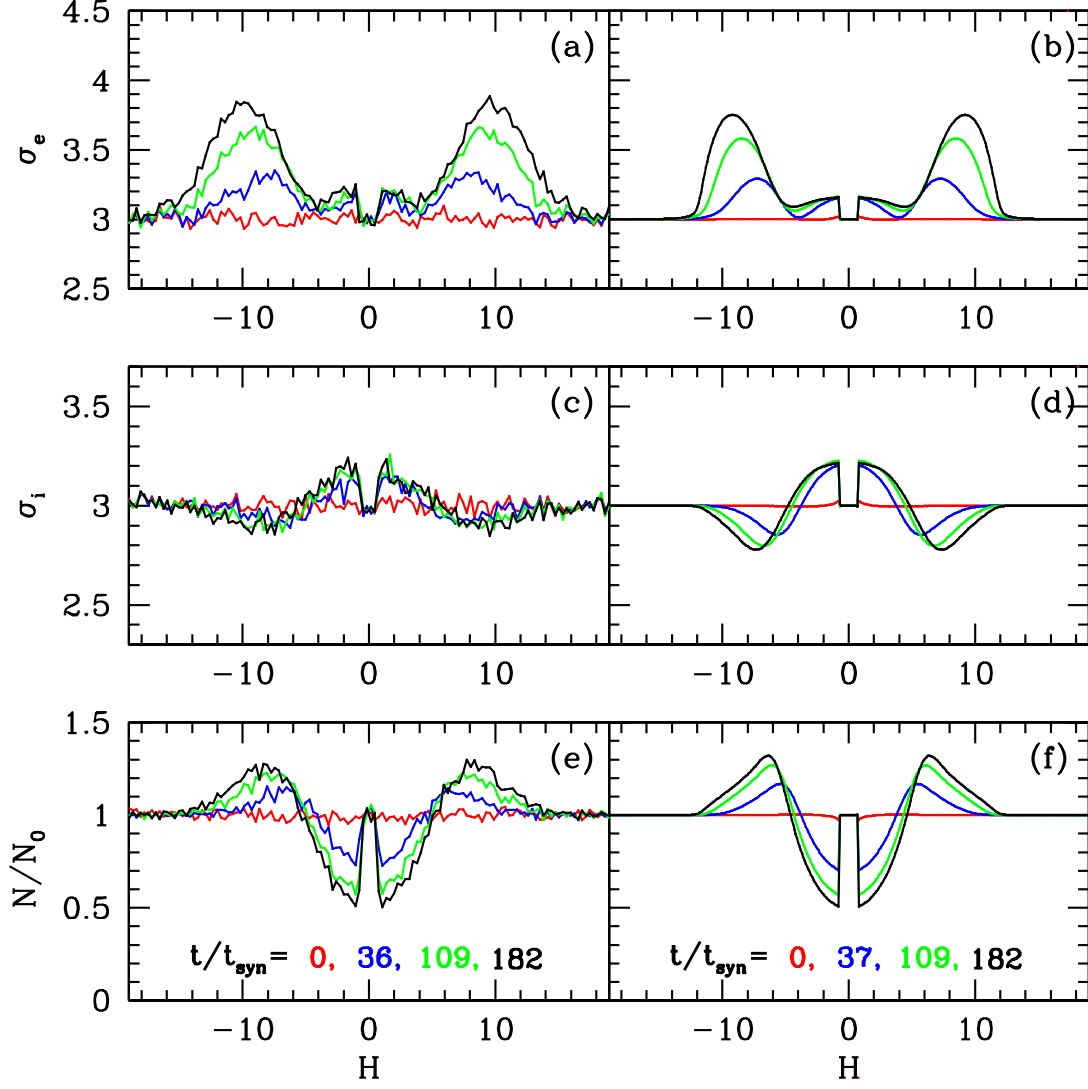


Fig. 5.— Evolution of the planetesimal disk properties driven by the presence of a massive protoplanetary embryo. Initially $\tilde{\sigma}_e = \tilde{\sigma}_i = 3$. The plots contain numerical (*left row*) and analytical (*right row*) time sequences of profiles of $\tilde{\sigma}_e$ (a,b), $\tilde{\sigma}_i$ (c,d), and dimensionless surface density normalized by its value at infinity (e,f). Curves of different colors represent profiles measured at specific moments of time normalized by the synodic period at a separation of $H = 1$ (which are shown in panels (e) and (f) by corresponding color coding; they are slightly different for numerical and analytical curves).

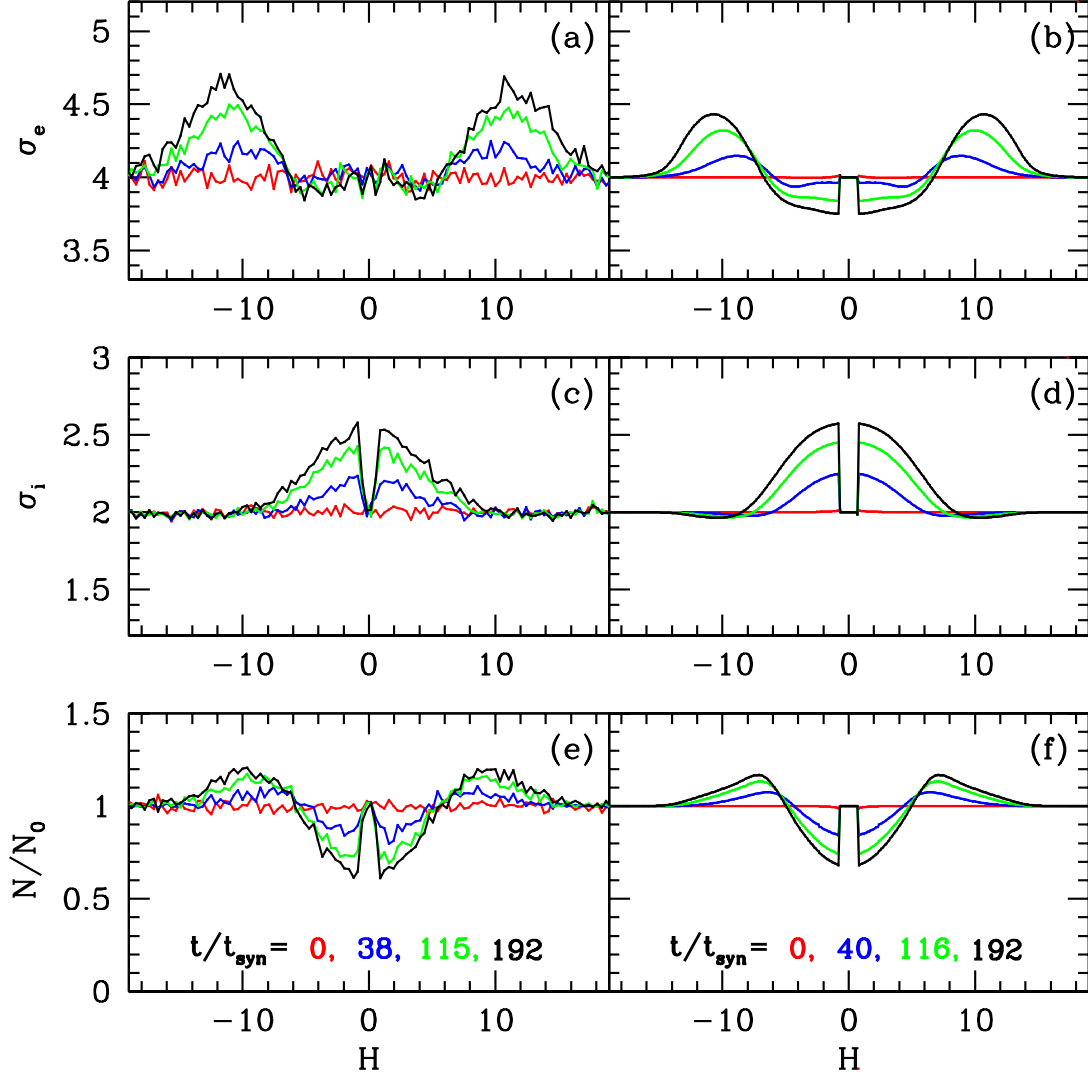


Fig. 6.— The same as Figure 5 but for initial $\tilde{\sigma}_e = 4, \tilde{\sigma}_i = 2$.

slightly smaller radial extent of the excited region than orbit integrations do (this might be caused by the effect of the distant encounters which theory can not reproduce very well, see Appendix B). In Figure 6 we display the same comparison of numerical and analytical results but now for the case of $\tilde{\sigma}_e = 4, \tilde{\sigma}_i = 2$. This corresponds to the ratio $\tilde{\sigma}_i/\tilde{\sigma}_e = 0.5$ which is within the range $0.45 - 0.55$ thought to be realized in homogeneous Keplerian planetesimal disks (Ida *et al.* 1993; Stewart & Ida 2000). One can see again a very good consistency between the two approaches, especially for the evolution of N and $\tilde{\sigma}_i$. There is a slight discrepancy between the predictions of two methods for the evolution of $\tilde{\sigma}_e$ near the horseshoe-passing orbits boundary. However, since equations (25)-(26) preserve the Jacobi constant one can be sure that the evolution of the surface density (which is driven by the redistribution of the angular momentum in the planetesimal disk) is always consistent with the evolution of epicyclic energy independent of the details of the spatial distributions of various quantities.

Planetesimals with the semimajor axes close to the embryo’s orbit perform horseshoe motion (see §3). As a result, surface density of guiding centers in this region stays constant in time as can be seen in Figures 5 and 6. Note that our orbit integrations do not exhibit the concentration of planetesimals at the embryo’s semimajor axis which is present in numerical calculations of Tanaka & Ida (1997). In their case this effect might have been caused by the analytical simplifications which were employed in Tanaka & Ida (1996, 1997) to speed up orbit integrations.

Figures 5 and 6 show that the embryo does not clear a complete gap on a dynamical timescale in the dispersion-dominated regime, although it does produce a significant depression in the surface density. Note that we plot the surface density of guiding centers of planetesimals N in Figures 5 and 6 rather than the instantaneous surface density. The depression formed in the instantaneous surface density at the location of the embryo is weaker than the gap in N because epicyclic motion allows planetesimals to penetrate inside the depression of N . The absence of a clear gap is due to the weakness of the individual embryo-planetesimal scattering in the dispersion-dominated regime. In the shear-dominated disk, scattering is much stronger and a gap is cleared by the embryo on a rather short timescale (see Paper I and Appendix B). It is also obvious that the evolution of the disk surface density is accompanied by a considerable change in kinematic properties of planetesimal population, as required by the conservation of Jacobi constant. Thus, the dynamical evolution of the disk is an important ingredient of the gap formation process which justifies the need for the self-consistent theory such as the one presented here.

The agreement between the analytical and numerical results in the dispersion-dominated regime is in general pretty good given the approximate nature of the theory and the small number of fitting parameters we are using — essentially only the constants in (20), (27), and (41) are free parameters, and it turns out that the solutions of equations (25)-(26) depend on their particular choice only very weakly. We believe that minor discrepancies between the outcomes of analytical and numerical approaches can be accounted for by going to the next order in $1/\ln \Lambda$ and properly including the effects of the distant encounters. We expect our analytical formulation to be even more accurate for larger values of $\tilde{\sigma}_e, \tilde{\sigma}_i$ but we have not investigated these because the compu-

tational requirements of the numerical simulations become prohibitive. We postpone the detailed exploration of these subjects for the future.

4. Embryo's accretion rate.

The accretion rate of planetesimals by the embryo \dot{M} is another observable (in addition to the spatial distributions of N , $\tilde{\sigma}_e$, and $\tilde{\sigma}_i$) which can be computed both analytically and numerically and used as a check of our calculations. In addition, it is a very important quantity by itself for any realistic modelling of planet formation. A lot of work has been devoted to the study of the planetary accretion in homogeneous planetesimal disks in the context of the planetary mass growth (Greenzweig & Lissauer 1990, 1992) and the origin of planetary spins and obliquities (Dones & Tremaine 1993). The results of these authors are not directly applicable to the inhomogeneous disks that are our primary focus but can be used as limiting cases to check our analytical predictions in the more general case of nonuniform distribution of planetesimals.

In Appendix C we calculate \dot{M} in different velocity regimes. In the dispersion-dominated case such a computation is made possible by the use of the two-body approximation and we find that

$$\dot{M} = m \frac{\Omega R_e^2}{8a_e^2} \int_{-\infty}^{\infty} N(H) \frac{|H| dH}{\tilde{\sigma}_e^2 \tilde{\sigma}_i^2} e^{-(H')^2/(2\tilde{\sigma}_e^2)} \left[\frac{(H')^2}{4} U_+(H', \tilde{\sigma}_e, \tilde{\sigma}_i) + \frac{2}{p} U_-(H', \tilde{\sigma}_e, \tilde{\sigma}_i) \right], \quad (42)$$

where

$$U_{\pm} = \int_0^{\infty} dr (1+r)^{\pm \frac{1}{2}} e^{-\frac{1}{2}(\alpha_e^2 + \alpha_i^2)r} I_0 \left[\frac{1}{2} (\alpha_i^2 - \alpha_e^2) r \right], \quad \alpha_e = \frac{H'/\tilde{\sigma}_e}{2\sqrt{2}}, \quad \alpha_i = \frac{H'/\tilde{\sigma}_i}{2\sqrt{2}}, \quad (43)$$

R_e is the embryo's physical radius, a_e is its semimajor axis, $p = R_e/R_H$, I_0 is a modified Bessel function of order zero, and $H'(H)$ is given by (27). Integration over dH in (42) should exclude the region $(-\tilde{h}_{hs}, \tilde{h}_{hs})$ corresponding to the horseshoe orbits.

In the shear-dominated regime we use simple scaling arguments to fix the accretion rate dependence on the physical variables of the system and find that

$$\dot{M} \approx 5N^{inst}(H_{coll}) \frac{m\Omega R_e R_H}{\langle \tilde{\sigma}_i \rangle a_e^2} \quad (44)$$

where $N^{inst}(H_{coll})$ is the surface density of planetesimals on orbits leading to collisions with the embryo (at $H = H_{coll} \approx 1.4$, see Appendix C), defined by equation (C10), and $\langle \tilde{\sigma}_i \rangle$ is a measure of $\tilde{\sigma}_i$ in the inhomogeneous disk obtained by averaging $\tilde{\sigma}_i$ over the interval $(-2R_H, 2R_H)$ [from where most of the planetesimals get accreted in the shear-dominated regime, see Petit & Hénon (1986)]. In Appendix B we demonstrate how to use these results to cover the regime of intermediate velocity dispersion.

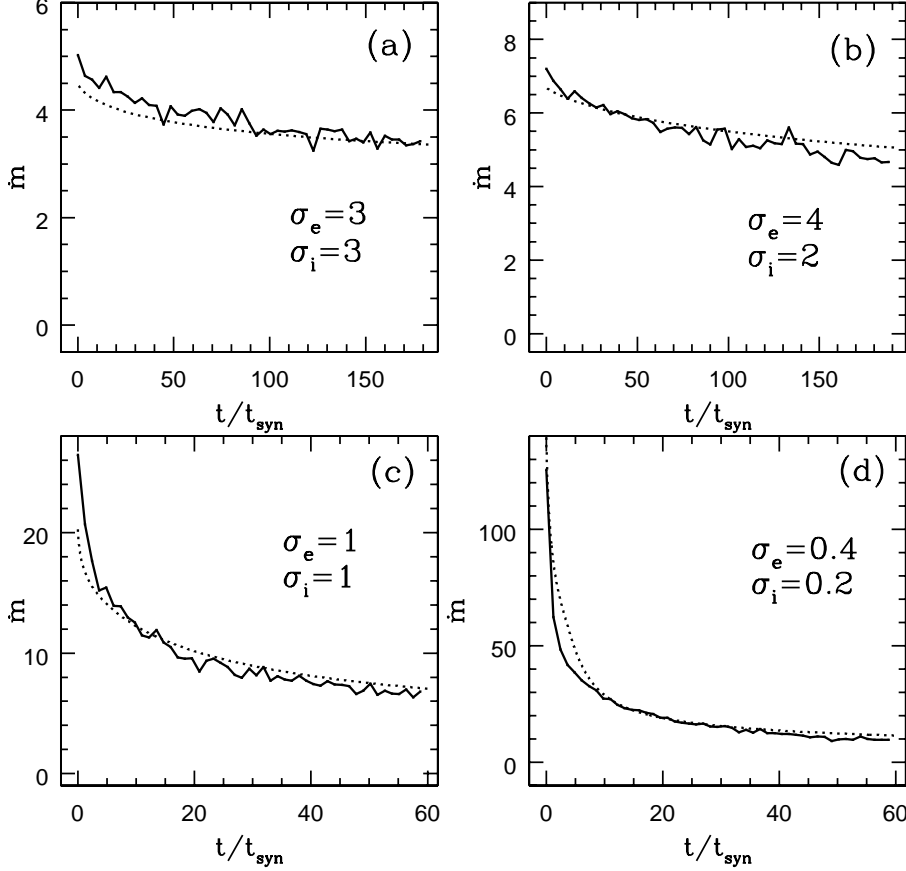


Fig. 7.— Dimensionless accretion rate $\dot{m} = \dot{M}/(\Omega R_e^2 \Sigma_0)$ (R_e is the radius of the planet, Σ_0 is the surface mass density of the disk far from the embryo) as a function of time (expressed in synodic periods t_{syn} at the separation of $1 R_H$) for different values of $\tilde{\sigma}_e$ and $\tilde{\sigma}_i$. Results of orbit integrations are shown by thick curve, and the dotted line shows analytical predictions. Accretion rates for the dispersion-dominated regime are presented in panels (a) and (b), while panels (c) and (d) display \dot{m} for intermediate velocity regime.

Figure 7 shows the comparison of our analytical predictions with the results of orbit integrations. We plot the dimensionless accretion rate $\dot{m} = \dot{M}/(\Omega R_e^2 \Sigma_0)$ (R_e is the radius of the planet, $\Sigma_0 = mN(\infty)/a_e^2$ is the dimensional surface mass density of the disk far from the embryo) as a function of time normalized by the synodic period t_{syn} corresponding to a separation of $1 R_H$ between the orbits of the embryo and planetesimal. Numerical accretion rates were computed during the calculation of the spatial and temporal evolution of various disk quantities described in §3.3.2. They are displayed by the thick solid line in Figure 7. Analytical results [using an interpolation given by formulae (B5) and (B6) where needed] are shown by a dotted line. One can see that the

agreement is reasonably good even in the intermediate velocity regime⁵ (Figure 7c,d). The theoretical results in the dispersion-dominated regime (Figure 7a,b) do not depend on the interpolation and their good agreement with the numerical accretion rates confirms the validity of the analytical approach developed in Appendix C. We will be using this prescription for the embryo’s accretion rate in upcoming work when dealing with the evolution of the planetesimal disk coupled to the embryo’s growth.

5. Direction of the embryo-planetesimal interaction.

From the results of the orbit integrations described in §3.3.2 one can see that the embryo-planetesimal interaction leads to a decrease in the surface density of planetesimals near the embryo in the region of passing orbits. The width of the surface density depression is typically of the order of the planetesimal eccentricity dispersion $\tilde{\sigma}_e$. At the same time the distribution of planetesimals on horseshoe orbits stays unaffected by the embryo.

This is very similar to the behavior of the surface density in the shear-dominated regime, as studied in Paper I. In that case the reason for such behavior was very clear: scattering of a planetesimal initially on a circular orbit can only increase its eccentricity and inclination which leads to the increase of $|H|$ (a result of Jacobi constant conservation) and, consequently, to the repulsion of planetesimal orbits. In Paper I planetesimals were kept on circular orbits at all times, and a gap with a width of several R_H was carved near the embryo’s orbit.

In the kinematically hot regime the reasoning is not so simple. From equation (28) and Figure 3 one can see that scattered planetesimals can have $\Delta|H| < 0$ as well as $\Delta|H| > 0$ for a fixed H depending on their eccentricities, inclinations, and epicyclic phases. Moreover, from our calculation of the scattering coefficients in the dispersion-dominated regime (Paper II, see also the analogous result in Ida *et al.* 2000) we know that $\langle \Delta\tilde{h} \rangle < 0$. Using this result Ida *et al.* (2000) suggested that in the kinematically hot planetesimal disk embryo should *attract* planetesimal orbits rather than *repel* them. The outcome of such an interaction would be a growth of planetesimal surface density at the embryo’s location.

However, this conclusion is misleading. What really determines the behavior of the planetesimal surface density near the embryo and the nature of the embryo-planetesimal interaction is the direction of the *flux* of planetesimals. The embryo repels planetesimals and carves a gap when this flux is directed away from the embryo; it attracts planetesimals and increases their nearby surface density when this flux is directed towards the embryo. The condition $\langle \Delta\tilde{h} \rangle < 0$ by itself cannot guarantee that the planetesimal flux is directed towards the embryo’s orbit because these

⁵Note that the specific form of interpolation function (B6) was chosen to fit several sets of $\tilde{\sigma}_e$ and $\tilde{\sigma}_i$, not only those displayed in Figure 7. In all studied cases numerical and analytical results agree within (10 – 30)%.

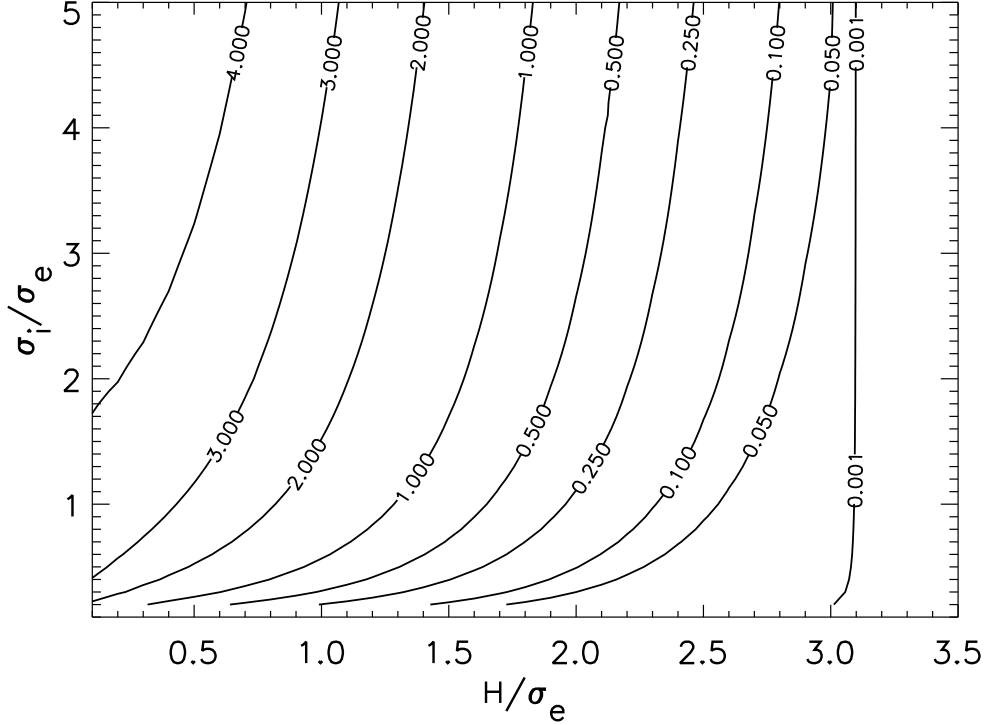


Fig. 8.— Contour plot of the dimensionless planetesimal flux $\pi\mathcal{F}/(|A|\mu_e^{1/3})$ as a function of $\tilde{\sigma}_i/\tilde{\sigma}_e$ — ratio of the vertical to horizontal velocity dispersions, and $H/\tilde{\sigma}_e$ — radial distance from the embryo scaled by the RMS epicyclic radius. Note that this flux is always positive for positive H meaning that the embryo *repels* planetesimals. The flux is an odd function of H .

quantities are not simply related⁶. Another complication precluding the use of the sign of $\langle\Delta\tilde{h}\rangle$ as an indicator of planetesimal disk evolution is that $\Delta H < 0$ (for $H > 0$) does not always mean that planetesimal orbit gets closer to the embryo. If for example $\Delta H < -2H$ then the absolute value of the semimajor axis separation after the encounter is larger than it was before, which is indicative of repulsion rather than attraction.

Using the method described in Appendix A of Paper I, we can calculate the outward flux of planetesimals \mathcal{F} driven by the embryo-planetesimal interactions. We evaluate this flux in a homogeneous disk. For the general scattering probability function $\tilde{P}(H_0, \Delta H)$ [$\tilde{P}(H_0, \Delta H)d\Delta H$ is the probability for a planetesimal initially at H_0 to have ΔH in the range $(\Delta H, \Delta H + d\Delta H)$] this

⁶One can imagine a scattering probability function which transports most of the planetesimals away from the embryo shifting them by a small $\Delta H > 0$; at the same time a small fraction of planetesimals can be scattered towards the embryo and have large negative values of ΔH . With properly chosen weights one can always ensure that $\langle\Delta\tilde{h}\rangle < 0$ while the bulk of material moves away from the embryo forming a gap around its orbit.

flux can be written as (see Papers I and II)

$$\mathcal{F} = \frac{|A|\mu_e^{1/3}}{\pi} \left[\int_0^\infty d(\Delta H) \int_{H-\Delta H}^H dH_0 |H_0| \tilde{P}(H_0, \Delta H) - \int_{-\infty}^0 d(\Delta H) \int_H^{H-\Delta H} dH_0 |H_0| \tilde{P}(H_0, \Delta H) \right]. \quad (45)$$

Differentiating this expression w.r.t. H gives us

$$\frac{\partial \mathcal{F}}{\partial H} = \frac{|A|\mu_e^{1/3}}{\pi} \left[|H| - \int_{-\infty}^\infty d(\Delta H) |H - \Delta H| \tilde{P}(H - \Delta H, \Delta H) \right]. \quad (46)$$

Since the planetesimal flux in a homogeneous disk has to vanish far from the embryo we can integrate (46) to obtain

$$\mathcal{F} = \frac{|A|\mu_e^{1/3}}{\pi} \int_{-\infty}^H dH_1 \left[|H_1| - \int_{-\infty}^\infty d(\Delta H) |H_1 - \Delta H| \tilde{P}(H_1 - \Delta H, \Delta H) \right]. \quad (47)$$

This expression [or (45)] is valid for an arbitrary function $\tilde{P}(H_0, \Delta H)$. In principle we can use this general form but it is more convenient to apply one of the most important properties of the interaction in the dispersion-dominated regime: that scattering is dominated by weak encounters, meaning that we can expand in (47) the integral in brackets in a Taylor series in ΔH . As a result, after some intermediate transformations we find that planetesimal flux in the initially homogeneous disk is given by

$$\mathcal{F}(H) = \frac{|A|\mu_e^{1/3}}{\pi} \left[|H| \langle \Delta \tilde{h} \rangle - \frac{1}{2} \frac{\partial}{\partial H} \left(|H| \langle (\Delta \tilde{h})^2 \rangle \right) \right]. \quad (48)$$

This expression could have also been obtained directly from equation (25) or (33). It is clear from the equation (48) why the sign of $\langle \Delta \tilde{h} \rangle$ cannot tell us the direction of the planetesimal evolution: the presence of additional term with the derivative of $|H| \langle (\Delta \tilde{h})^2 \rangle$ in r.h.s. of (48) which cannot in general be related⁷ to $\langle \Delta \tilde{h} \rangle$ means that there is no direct relation between the signs of $\mathcal{F}(H)$ and $\langle \Delta \tilde{h} \rangle$.

Using the analytical formulae for $\langle \Delta \tilde{h} \rangle$ and $\langle (\Delta \tilde{h})^2 \rangle$ derived in Paper II, we can calculate this flux in the Fokker-Planck approximation as a function of distance from the embryo and the ratio of the vertical to horizontal velocity dispersions. The result of such a calculation is presented in Figure 8. The shape of the contours is universal in the coordinates $H/\tilde{\sigma}_e, \tilde{\sigma}_i/\tilde{\sigma}_e$, i.e. it does not depend on the embryo mass, planetesimal mass, or other parameters. In plotting \mathcal{F} we have also

⁷A relation between the first and second order diffusion coefficients exists if a homogeneous distribution is a steady-state solution of the Fokker-Planck equation see Lifshitz & Pitaevskii (1981). In our case this is not true — embryo's gravity tends to make disk inhomogeneous by carving out a gap.

neglected the effect of interaction at large azimuthal distances near the horseshoe region boundary described in §3.3 (it can be easily taken into account and will only slightly shift the contours near $H \sim 1$.) One can easily see from Figure 8 that $\mathcal{F} > 0$ when $H > 0$ for all values of $H/\tilde{\sigma}_e$ and $\tilde{\sigma}_i/\tilde{\sigma}_e$ which we explored (and $\mathcal{F} < 0$ for $H < 0$ by symmetry). This implies that the embryo tends to *repel* planetesimals by driving a flux directed away from its orbit. This conclusion disagrees with the predictions based on the sign of $\langle \Delta \tilde{h} \rangle$ (Ida *et al.* 2000). The planetesimal flux vanishes as $H/\tilde{\sigma}_e$ grows but distant encounters (not included in Figure 8) will dominate at large $H/\tilde{\sigma}_e$ and they also always drive planetesimals away from the embryo (Goldreich & Tremaine 1982; Petit & Hénon 1987a). Thus, it appears that repulsion is the only possible outcome of the embryo-planetesimal gravitational interaction even in the dispersion-dominated velocity regime.

Figure 8 seems to imply that the planetesimal surface density will always grow because \mathcal{F} decreases with H . This is not the case because the boundary condition (38) forces $\mathcal{F} = 0$ at the horseshoe-passing orbit boundary $H = \tilde{h}_{hs}$. This means that there is actually a transition zone near $H = \pm \tilde{h}_{hs}$ in which flux steeply increases from 0 to its value given by (48). The width of this zone is infinitesimal initially but it rapidly expands as the planetesimal disk evolves under the action of the embryo’s gravity. Within the transition region \mathcal{F} is positive and increases with H meaning that the planetesimal surface density decays there. This is exactly what was observed in the analytical calculations and numerical orbit integrations in §3.3.2. The slowdown of the disk evolution obvious from Figures 5 and 6 is caused not only by the growth of epicyclic energy of the disk (which lengthens the disk dynamical timescale) but also by the gradual expansion of the transition zone leading to a decrease in the planetesimal flux gradient and slower disk evolution.

6. Discussion and conclusions.

We have studied the embryo-planetesimal interaction in the gravitational field of a central star. Two different cases were explored: when the interaction between the embryo and planetesimals occurs in the shear-dominated and in the dispersion-dominated regimes. The treatment of the first case parallels that of Paper I but is complicated by the fact that now we explicitly include the evolution of not only the surface density but also the eccentricity and inclination of planetesimals in the disk.

Our study of the dispersion-dominated regime relies on the methods of kinetic theory, and it uses many of the results obtained in Paper II. However our present treatment is more refined since the description of embryo-planetesimal scattering requires clarifying many details which were not important for the planetesimal-planetesimal interactions. In particular we have to study not only passing but also horseshoe orbits of planetesimals to determine the spatial distribution of the disk properties. To do this we propose a condition which separates the horseshoe and passing orbits and check its viability using numerical orbit integrations. Angular momentum exchange between the embryo and planetesimal long before and after their closest approach turns out to be important for the scattering on passing orbits near the horseshoe boundary. We illustrate this point by comparing

the analytical scattering probability function with the one obtained from numerical integrations. A simple method to account for this effect in our Fokker-Planck approach is proposed. Taken together all these refinements are shown to provide rather good agreement with the results of the numerical orbit integrations. Thus we hope to have grasped the most important features of the embryo-planetesimal interaction by our theoretical approach.

This does not mean that our treatment of the embryo-planetesimal interaction is complete. We have only focussed on the most important, dominant effects, and there is certainly room for additional refinements, which would farther improve the agreement with numerical results. The calculation of the scattering coefficients to the next order in $1/\ln \Lambda$ would provide us with subdominant corrections which might be important for modest values of $\tilde{\sigma}_e$ and $\tilde{\sigma}_i$. One can certainly do a better job in treating distant encounters, calculating various coefficients entering formulae (20), (27), etc. or the interpolating functions of Appendix B, using a larger set of numerical orbit integrations. On a somewhat deeper level, one can try to come up with a more sophisticated treatment of the horseshoe-passing orbits separation (instead of the complete spatial separation of these two types of orbits assumed in this paper). Our purely deterministic treatment of the shear-dominated regime can also be improved, which would ameliorate the comparison with numerical results in the intermediate velocity regime (see Appendix B). The recoil of the embryo and the excitation of the embryo’s eccentricity and inclination in the course of the planetesimal gravitational scattering can be important in some applications, such as the embryo’s migration (Tanaka & Ida 1999) or its interaction with the embryos nearby (Tanaka & Ida 1997). Our treatment relies on the use of the Schwarzschild velocity distribution which was demonstrated to be applicable in the dispersion-dominated regime (Greenzweig & Lissauer 1992), but the deviations from this assumption could be important e.g. in the intermediate velocity regime, and this subject can also be pursued farther. All these refinements would better the quantitative agreement between the analytical theory and numerical results. But reasonably good accord is provided even by our basic treatment developed here, especially in the dispersion-dominated case where the assumptions we make are the most justifiable.

We also dwell upon the question of the direction of the embryo-planetesimal interaction, namely whether it leads to the repulsion of planetesimal orbits from the embryo or to their attraction. The latter outcome has been favored in some scenarios (Ida *et al.* 2000) and is based on the fact that in the dispersion-dominated regime embryo *on average* tends to attract planetesimal semimajor axes toward its orbit. We demonstrate, however, that the average change of planetesimal semimajor axes cannot serve a standard for determining the direction of the embryo-planetesimal interaction because the transport of the angular momentum (associated with the changes in semimajor axes) is not the same as the bulk motion of the disk material. We propose our own criterion for judging the embryo-planetesimal scattering outcome, and show that the embryo always *repels* planetesimals rather than attracts them in an initially homogeneous disk thereby carving out a gap in the distribution of the planetesimal semimajor axes [which is in contrast to claims by Ida *et al.* (2000)]. Our own numerical results support this conclusion.

The combination of our results for planetesimal-planetesimal gravitational scattering presented in Paper II and the theory for the embryo-planetesimal interaction developed here now allows us to study the planetesimal disk dynamics with these processes operating simultaneously. It also provides a framework to which various refinements and additional physical mechanisms can be naturally added. Our results are not restricted in applications to the problem of the formation of planetary systems but can also be used for studying their present day evolution, e.g. the dynamics of asteroid and Kuiper belts affected by massive bodies inside or near them. Our results for the accretion rate of massive body immersed in inhomogeneous planetesimal disk (§4 & Appendix C) allow us also to include self-consistently the embryo’s mass growth into consideration. We will examine protoplanetary disk evolution with all these effects working together in a future work (Rafikov 2002b).

I am grateful to my advisor, Scott Tremaine, for his patient guidance and valuable advice. The financial support of this work by the Charlotte Elizabeth Procter Fellowship and NASA grant NAG5-10456 is thankfully acknowledged.

REFERENCES

- Binney, J. & Tremaine, S. 1987 , *Galactic Dynamics*, Princeton University Press
- Bryden, G., Lin, D. N. C., & Ida, S. 2000, ApJ, 544, 481
- Dones, L. & Tremaine, S. 1993, Icarus, 103, 67
- Goldreich, P. & Tremaine, S. 1980, ApJ, 241, 425
- Goodman, J. 1983, ApJ, 270, 700
- Goodman, J. 1985, in *Dynamics of Star Clusters*, eds. J. Goodman & P. Hut, 179
- Gradshteyn, I.S. & Ryzhik, I.M. 1980, *Table of integrals, series, and products*, New York: Academic Press
- Greenzweig, Y. & Lissauer, J. J. 1990, Icarus, 87, 40
- Greenzweig, Y. & Lissauer, J. J. 1992, Icarus, 100, 440
- Hasegawa, M. & Nakazawa, K. 1990, A&A, 227, 619
- Hénon, M. & Petit, J.M. 1986, Celestial Mechanics, 38, 67
- Ida, S. 1990, Icarus, 88, 129
- Ida, S., Bryden, G., Lin, D. N. C., & Tanaka, H. 2000, ApJ, 534, 428

- Ida, S., Kokubo, E., & Makino, J. 1993, MNRAS, 263, 875
- Ida, S. & Makino, J. 1993, Icarus, 106, 210
- Ida, S. & Nakazawa, K. 1989, A&A, 224, 303
- Landau, L. D. & Lifshitz, E. M. 1989, *Mechanics*; New York: Pergamon Press
- Lifshitz, E. M. & Pitaevskii, L. P. 1981, *Physical kinetics*; New York: Pergamon Press
- Murray, C. D. & Dermott, S. F. *Solar System Dynamics*; Cambridge University Press, 1999
- Namouni, F. 1999, Icarus, 137, 293
- Ohtsuki, K. & Tanaka, H. 2002, submitted to Icarus
- Petit, J.M. & Hénon, M. 1986, Icarus, 66, 536
- Petit, J.M. & Hénon, M. 1987a, A&A, 173, 389
- Petit, J.M. & Hénon, M. 1987b, A&A, 188, 198
- Petit, J.M. & Hénon, M. 1988, A&A, 199, 343
- Press, W. H. *et al. Numerical Recipes in C*; Cambridge University Press, 1988
- Rafikov, R.R. 2001, AJ, 122, 2713, Paper I
- Rafikov, R.R. 2002a, submitted to AJ, Paper II
- Rafikov, R.R. 2002b, submitted to AJ
- Stewart, G. R. & Ida, S. 2000, Icarus, 143, 28
- Stewart, G. R. & Wetherill, G. W. 1988, Icarus, 74, 542
- Tanaka, H., & Ida, S. 1996, Icarus, 120, 371
- Tanaka, H., & Ida, S. 1997, Icarus, 125, 302
- Tanaka, H., & Ida, S., 1999, Icarus, 139, 350
- Wetherill, G. W. & Stewart, G. R. 1989, Icarus, 77, 330
- Wetherill, G. W. & Stewart, G. R. 1993, Icarus, 106, 190

A. Scattering probability function in the dispersion-dominated regime.

In this appendix we calculate the scattering distribution function $\tilde{P}(H, \Delta H)$ in the dispersion-dominated regime. This function is defined such that $\tilde{P}(H, \Delta H)d(\Delta H)$ is the probability that two bodies initially separated by H will have a change of H in the interval $(\Delta H, \Delta H + d(\Delta H))$ during an encounter. This probability will initially be considered as a function of also \tilde{e} and \tilde{i} . Then we will average it over the distribution of \tilde{e} and \tilde{i} and obtain the averaged value of $\tilde{P}(H, \Delta H)$ as a function of $\tilde{\sigma}_e$ and $\tilde{\sigma}_i$. We will extensively use the results and notation of §4 of Paper II which should be consulted for further details and clarifications.

To do this we will employ the two-body approximation. We first relate ΔH to the change of the relative velocity in the y -direction Δv_y using formula $\Delta H = 2\Delta v_y/(\Omega R_H)$. Then we switch to the coordinates l (impact parameter) and ϕ (angle in the plane perpendicular to the direction of approach velocity⁸) to characterize the trajectory of the bodies. Using these coordinates one can express Δv_y as (Binney & Tremaine 1987)

$$\Delta v_y = -\Delta v_{\parallel} \frac{v_y}{v} + \Delta v_{\perp} \frac{\sqrt{v_x^2 + v_z^2}}{v} \cos \phi, \quad (\text{A1})$$

where v_x, v_y, v_z and v are different components of the planetesimal approach velocity and its magnitude given by equations (58) and (60) of Paper II; expressions for Δv_{\parallel} and Δv_{\perp} are given by (67) *ibid.* This allows us to express ΔH as

$$\Delta H = \frac{2}{1 + (l/l_0)^2} [-H + 2(l/l_0) \tilde{v}_1 \cos \phi]. \quad (\text{A2})$$

where $\tilde{v}_1^2 = \tilde{e}^2 + \tilde{i}^2 - H^2$ (\tilde{v}_1^2 is always positive because $|H| < \tilde{e}$ for the kind of scattering we consider here) and $l_0 = G(m_1 + m_2)/v^2 = R_H(\Omega r_H/v)^2$ (when minimum approach distance between interacting bodies $\leq l_0$ large-angle two-body scattering takes place).

For a fixed ΔH this equation can be rewritten as an equation for $u = (l/l_0) \cos \phi$ and $w = (l/l_0) \sin \phi$:

$$\left(u - \frac{2\tilde{v}_1}{\Delta H}\right)^2 + w^2 = R^2, \quad R^2 = \frac{(\Delta H - \Delta H_-)(\Delta H_+ - \Delta H)}{\Delta H^2}, \quad (\text{A3})$$

where

$$\Delta H_- = -H - \sqrt{H^2 + 4\tilde{v}_1^2}, \quad \Delta H_+ = -H + \sqrt{H^2 + 4\tilde{v}_1^2}. \quad (\text{A4})$$

Clearly this is only possible if

$$\Delta H_- < \Delta H < \Delta H_+. \quad (\text{A5})$$

⁸The origin from which this angle is counted is not important here.

Thus, the difference in planetesimal semimajor axes cannot increase by more than ΔH_+ or decrease by more than ΔH_- during the scattering. Equation (A3) is simply the equation of a shifted circle with radius R in coordinates u, w .

To calculate the probability distribution function $\tilde{P}(H, \Delta H)$ we use the following identity:

$$\tilde{P}(H, \Delta H) = \begin{cases} \left. \frac{d}{dz} \tilde{P}(H, \Delta H' < z) \right|_{z=\Delta H}, & \Delta H < 0, \\ -\left. \frac{d}{dz} \tilde{P}(H, \Delta H' > z) \right|_{z=\Delta H}, & \Delta H > 0, \end{cases} \quad (\text{A6})$$

where $\tilde{P}(H, \Delta H' < z)$ and $\tilde{P}(H, \Delta H' > z)$ are complementary cumulative probability distributions. We calculate them in the following way.

It is clear that the probability $\tilde{P}(H, \mathbf{S})$ of some outcome of scattering is equal to the ratio of the area of the region of the space of epicyclic phases $\tau - \omega$ corresponding to the outcome manifold \mathbf{S} and $4\pi^2$. Using the conversion between the integration over $\tau - \omega$ and $l - \phi$ represented by equation (61) of Paper II we can write this as

$$\tilde{P}(H, \mathbf{S}) = \int_{\mathbf{S}} \frac{d\tau d\omega}{4\pi^2} = \frac{4}{3\pi} \frac{1}{R_H^2} \frac{v}{\Omega R_H} \frac{1}{\tilde{i}|H|\sqrt{\tilde{e}^2 - H^2}} \int_{\mathbf{S}} l dl \frac{d\phi}{2\pi}. \quad (\text{A7})$$

Thus we can always transform our problem into the calculation of the area of region \mathbf{S} in $l - \phi$ coordinates. Here we are interested in the area of the region given by $\Delta H < z$ for $z < 0$ and by $\Delta H > z$ for $z > 0$.

One can easily see that both conditions correspond to the inner part of a circle given by equation (A3). Thus the area of the region in $l - \phi$ phase space bounded by these conditions is always represented by a single formula (no matter whether z is positive or negative):

$$\int_{\mathbf{S}} l dl \frac{d\phi}{2\pi} = \frac{\pi R^2}{2\pi} = \frac{l_0^2}{2} \frac{(z - \Delta H_-)(\Delta H_+ - z)}{z^2}. \quad (\text{A8})$$

Substituting this result into (A7) and then into (A6) we obtain (using the definitions of v and l_0) that

$$\tilde{P}(H, \Delta H) = \frac{4}{3\pi} \frac{4\tilde{v}_1^2 - H\Delta H}{|\Delta H|^3} \frac{1}{\tilde{i}|H|\sqrt{\tilde{e}^2 - H^2} [\tilde{e}^2 + \tilde{i}^2 - (3/4)H^2]^{3/2}} \quad (\text{A9})$$

if $\Delta H_- < \Delta H < \Delta H_+$, and $\tilde{P}(H, \Delta H) = 0$ otherwise. Recalling the definition of \tilde{v}_1^2 and using the definitions of scattering coefficients $\langle \Delta \tilde{h} \rangle_{\tau, \omega}$ and $\langle (\Delta \tilde{h})^2 \rangle_{\tau, \omega}$ given by equations (73), (74), and (77) of Paper II we can rewrite (A9) in a more appealing form:

$$\tilde{P}(H, \tilde{e}, \tilde{i}, \Delta H) = \frac{1}{2 \ln \Lambda} \frac{\langle (\Delta \tilde{h})^2 \rangle_{\tau, \omega} + \langle \Delta \tilde{h} \rangle_{\tau, \omega} \Delta H}{|\Delta H|^3}, \quad (\text{A10})$$

where the dependence on \tilde{e} and \tilde{i} is hidden in $\langle \Delta \tilde{h} \rangle_{\tau, \omega}$ and $\langle (\Delta \tilde{h})^2 \rangle_{\tau, \omega}$.

The expression for the differential probability given by equation (A10) is most accurate for large angle scattering (i.e. for $\Delta H \gtrsim 1$) because this means very small impact parameters implying that the two-body scattering assumption is very good. This allows one to use this probability function to study strong scattering in the Hill approximation. On the other hand when $\Delta H \rightarrow 0$ the expression (A10) clearly diverges. This divergence is unphysical because the two-body assumption becomes very bad there. Small ΔH means weak scattering which only occurs for large impact parameters l . In real planetesimal disks l is always restricted to be $\lesssim \tilde{i}R_H$. Thus our formula (A10) is only applicable for $|\Delta H| \gtrsim \Delta H_{min}$, where we find ΔH_{min} by setting $l \approx \tilde{i}R_H \gg l_0$ in equation (A2):

$$\Delta H_{min} \approx \frac{2\tilde{v}_1}{\tilde{i}} \left(\frac{\Omega R_H}{v} \right)^2 \ll 1. \quad (\text{A11})$$

When $|\Delta H| \lesssim \Delta H_{min}$ the scaling provided by (A10) is not applicable and the probability distribution of scattering assumes some different form. However, in most cases we need not worry about the effects of this indeterminacy for small ΔH because usually we need only the integrated characteristics of the probability function [e.g. in calculation of some scattering coefficients in Paper II which could be done using $\tilde{P}(H, \Delta H)$, see below]. Integrals of $\tilde{P}(H, \Delta H)$ are subject to strong cancellation effects near $\Delta H = 0$ and this naturally removes the problem. Similar situation was discussed by Goodman (1983, 1985) in the context of stellar gravitational encounters in globular clusters.

Using (A9) we can provide an alternative derivation of $\langle \Delta \tilde{h} \rangle_{\tau, \omega}$. Multiplying r.h.s. of (A9) by ΔH and integrating from ΔH_- to $-\Delta H_{min}$ and from ΔH_{min} to ΔH_+ one obtains that⁹

$$\langle \Delta \tilde{h} \rangle_{\tau, \omega} = -\frac{4}{3\pi} \frac{\tilde{h} \ln(|\Delta H_-| |\Delta H_+| / \Delta H_{min}^2)}{\tilde{i} |H| \sqrt{\tilde{e}^2 - H^2} [\tilde{e}^2 + \tilde{i}^2 - (3/4)H^2]^{3/2}}. \quad (\text{A12})$$

Using (A4) and (A11) we find that

$$\ln \left(\frac{|\Delta H_-| |\Delta H_+|}{\Delta H_{min}^2} \right) = 2 \ln \left(\tilde{i} \frac{v^2}{\Omega^2 R_H^2} \right) = 2 \ln \Lambda, \quad (\text{A13})$$

which means that expression (A12) coincides with equation (73) of Paper II.

For some purposes it will still be necessary to use the distribution probability (A10) itself rather than its integrals. For these occasions we can remedy the divergence in (A10) by introducing some cutoff distance $d \sim \Delta H_{min}$ into the denominator of (A10). One can do this in a variety of ways, one of the simplest ones would be to take

$$\tilde{P}(H, \tilde{e}, \tilde{i}, \Delta H) = \frac{1}{2 \ln \Lambda} \frac{\langle (\Delta \tilde{h})^2 \rangle_{\tau, \omega} + \langle \Delta \tilde{h} \rangle_{\tau, \omega} \Delta H}{(|\Delta H| + d)^3}. \quad (\text{A14})$$

⁹Remember that we are using $\langle \Delta \tilde{h} \rangle$ and $\langle (\Delta \tilde{h})^2 \rangle$ instead of $\langle \Delta H \rangle$ and $\langle (\Delta H)^2 \rangle$ for consistency with the notation of Paper II.

One can easily check that the normalization of the total probability to 1 would require that

$$d \approx \left[\frac{\langle (\Delta \tilde{h})^2 \rangle_{\tau, \omega}}{2 \ln \Lambda} \right]^{1/2}. \quad (\text{A15})$$

We use this nondivergent form of (A14) in §3.3.

To take into account the distribution of planetesimal eccentricities and inclinations we need to average the differential probability using Schwarzschild velocity distribution. Expression (A10) provides a natural way of doing this and we find as a result that

$$\tilde{P}(H, \tilde{\sigma}_e, \tilde{\sigma}_i, \Delta H) = \frac{1}{2 \ln \Lambda} \frac{\langle (\Delta \tilde{h})^2 \rangle + \langle \Delta \tilde{h} \rangle \Delta H}{|\Delta H|^3}, \quad (\text{A16})$$

where explicit analytic expressions for $\langle \Delta \tilde{h} \rangle$ and $\langle (\Delta \tilde{h})^2 \rangle$ are given by equations (86) and (87) of Paper II. In principle we should be bearing in mind the restriction (A5) when doing this last averaging. In practice this can only slightly affect the factor inside the logarithm if we restrict the range of ΔH by approximate condition

$$\Delta \hat{H}_- < \Delta H < \Delta \hat{H}_+, \quad \Delta \hat{H}_{\pm} = -H \pm \sqrt{H^2 + 4(\tilde{\sigma}_e^2 + \tilde{\sigma}_i^2 - H^2)}. \quad (\text{A17})$$

Outside of this range simple form (A16) will give rather poor approximation. The nondivergent form of (A16) can be obtained in the same fashion as (A14) and (A15).

B. Intermediate velocity regime and distant encounters.

Equations (13)-(15) and (25)-(26) describe the evolution of the disk properties in the shear- and dispersion-dominated regimes correspondingly. Unfortunately the assumptions we have made while deriving them preclude us from using these equations directly in the intermediate regime, when

$$\tilde{\sigma}_e^2 + \tilde{\sigma}_i^2 \sim 1. \quad (\text{B1})$$

Still we can try to provide an approximate description of evolution in this velocity regime by smoothly interpolating between the two extremes we believe we can describe well. Of course, one should not expect very good agreement of the theory interpolated into the intermediate velocity regime with the outcomes of orbit integrations. Qualitative concord would be enough for our purposes.

Far from the embryo where the scattering due to close encounters is exponentially small (because of the scarcity of planetesimals with large eccentricities) distant encounters dominate the evolution of the planetesimal disk because their effect decays only as a power law in the embryo-planetesimal separation. We attempt to take them into account by using the same interpolation

technique: we assume that when $H/\tilde{\sigma}_e \ll 1$ close encounters dominate and scattering is described by formulae of §3.3. When $H/\tilde{\sigma}_e \gg 1$ distant encounters dominate and we use formulae of §3.2 to describe their effect on the disk properties because distant scattering is similar to the shear-dominated scattering.

To provide a smooth matching between the different velocity regimes and spatial scattering zones we use interpolating functions $\Theta(x)$ and $\Psi(x)$ with the following properties: $\Theta(x), \Psi(x) \rightarrow 0$ as $x \rightarrow 0$ and $\Theta(x), \Psi(x) \rightarrow 1$ as $x \gg 1$. Then we can describe evolution of some quantity $F(N, \tilde{\sigma}_e^2, \tilde{\sigma}_i^2)$ in terms of the corresponding shear- and dispersion-dominated extremes as

$$\frac{\partial F}{\partial t} = \Theta(\tilde{\sigma}_e^2 + \tilde{\sigma}_i^2) \left. \frac{\partial F}{\partial t} \right|_{disp} + [1 - \Theta(\tilde{\sigma}_e^2 + \tilde{\sigma}_i^2) (1 - \Psi(H/\tilde{\sigma}_e))] \left. \frac{\partial F}{\partial t} \right|_{shear}. \quad (\text{B2})$$

The properties of $\Theta(x)$ and $\Psi(x)$ ensure that this formula reproduces correct limiting behaviors of disk evolution.

We have found that the results of orbit integrations performed in the intermediate velocity regime can be satisfactorily described using the following form of interpolating function $\Theta(x)$:

$$\Theta(x) = \exp \left[-\frac{40}{x^{1/2}(5+x)^3} \right]. \quad (\text{B3})$$

For $\Psi(x)$ we use the following *ad hoc* prescription:

$$\Psi(x) = \exp \left[-(8/x)^4 \right]. \quad (\text{B4})$$

Comparison of the disk evolution in the intermediate regime computed using equations (B2)-(B4) with that obtained from direct orbit integrations is shown in Figure 9. We display the results for a disk with initial $\tilde{\sigma}_e = \tilde{\sigma}_i = 1$. One can see that the agreement between two methods is only qualitative indeed. The most probable reason for this is the use of the simple prescription (13)-(15) with a discrete probability function (12) to treat the shear-dominated regime. This also rules out the possibility of accurate treatment of the effects of distant encounters. In fact, as long as the random motion in the disk is not exactly zero scattering always has some dispersion of outcomes and this gives rise to the diffusive transport of planetesimals in the disk. Inclusion of this effect would widen and lower the surface density profile as well as remove spiky features caused by the discrete scattering function (12). We do not pursue this subject here and leave its detailed exploration for the future. Still, we have verified using several different choices of $\tilde{\sigma}_e$ and $\tilde{\sigma}_i$ in the intermediate velocity regime that qualitative agreement is adequate: general features and trends appearing in the numerical results are always reproduced reasonably well by our analytical prescription.

In Appendix C we describe the calculation of the planetesimal accretion by the embryo in the shear- and dispersion-dominated regimes. We again use the interpolation approach for the description of the accretion rate in the intermediate velocity regime:

$$\dot{M} = \Pi(\tilde{\sigma}_e^2 + \tilde{\sigma}_i^2) \dot{M}_{disp} + [1 - \Pi(\tilde{\sigma}_e^2 + \tilde{\sigma}_i^2)] \dot{M}_{shear}, \quad (\text{B5})$$

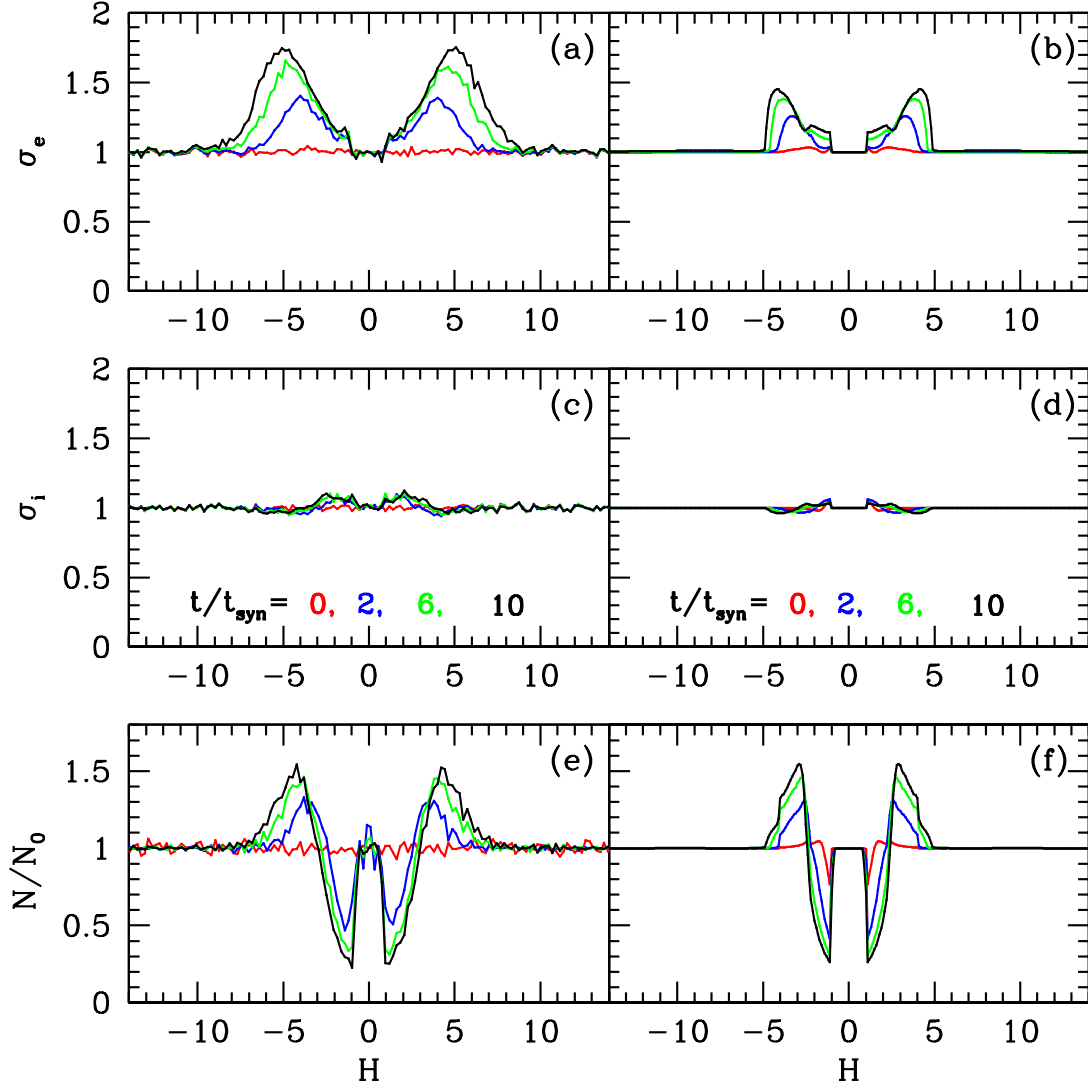


Fig. 9.— The same as Figure 5 but for initial $\tilde{\sigma}_e = \tilde{\sigma}_i = 1$. Dimensionless time is displayed in panels (c,d).

where \dot{M}_{disp} is given by (42), \dot{M}_{shear} by (44), and function $\Pi(x)$ has the same properties as $\Theta(x)$ and $\Psi(x)$. We have chosen¹⁰

$$\Pi(x) = \exp \left[-\frac{1}{(2.8x)^{1.45}} \right]. \quad (\text{B6})$$

Comparison of theoretical mass accretion rates obtained using (B5) with those derived from the orbit integrations in the intermediate dispersion regime is shown in Figure 7c,d.

C. Embryo accretion rate in an inhomogeneous planetesimal disk.

The accretion rate of any massive body immersed in a planetesimal disk depends sensitively on the dynamical state of the disk. Detailed studies of various accretion regimes in homogeneous disks were carried out by a number of authors (Greenzweig & Lissauer 1990, 1992; Dones & Tremaine 1993) and we will use some of their results.

We will concentrate on one very important regime: when the maximum planetesimal impact parameter l_{max} necessary for accretion to take place is much smaller than the disk vertical scale-height. If this condition is not fulfilled the inclination of planetesimals must be unrealistically small (Dones & Tremaine 1993),

$$\tilde{\sigma}_i \leq p, \quad p = \frac{R_e}{R_H}. \quad (\text{C1})$$

The dimensionless parameter p is the ratio of the embryo's radius R_e to its Hill radius R_H . It is independent of the mass of the accretor and is typically rather small in the Solar system ($< 10^{-2}$).

In the dispersion-dominated regime, when $\tilde{\sigma}_e^2 + \tilde{\sigma}_i^2 \gg 1$ [this is the 3-dimensional high-dispersion regime of Dones & Tremaine (1993)], analytical treatment of the accretion rate is possible, because the two-body approximation is valid in this velocity regime (see Paper II). In this approximation the accretion cross-section is

$$S = \pi R_e^2 \left[1 + \frac{2G(M_e + m)}{R_e v^2} \right], \quad (\text{C2})$$

where M_e and m are accretor and planetesimal masses, and v is the approach velocity of the planetesimal particles at infinity. The second term in this formula takes into account gravitational focussing, which is very important in planetesimal disks.

We proceed in a manner analogous of that of Paper II (see §4). We first fix H , \tilde{e} , and \tilde{i} of planetesimals. Only planetesimals with $|H| < \tilde{e}$ can experience close encounters with the embryo and be accreted. In addition, planetesimals on horseshoe orbits cannot be accreted either, thus we

¹⁰This choice of $\Pi(x)$ certainly depends on the accuracy of formula (C9) and our specific value of H_{coll} , see Appendix C.

put another restriction on H : $|H| > \tilde{h}_{hs}$, with \tilde{h}_{hs} given by (22). Also, following the discussion in §3.3, we need to distinguish the value of the semimajor axis difference immediately before the encounter H' from its value at infinity, H . The conservation of planetesimal flux means that the surface number densities of planetesimals immediately before the encounter N' and far from the embryo N are related via

$$N'(H')|H'|dH' = N(H)|H|dH. \quad (C3)$$

If the dependence $H'(H)$ is given by our simple approximation (27) then $dH'/dH = H/H'$ and $N'(H'(H)) = N(H)$; of course this would not be true for any other relation between these quantities.

The total number of planetesimals with semimajor axes between H and $H + dH$, eccentricities and inclinations in the intervals $[\tilde{e}, \tilde{e} + d\tilde{e}]$ and $[\tilde{i}, \tilde{i} + d\tilde{i}]$ correspondingly passing the accretor in a unit of time is

$$\delta N = \frac{3}{2}\Omega \frac{R_H^2}{a_e^2} N(H) \psi(\tilde{e}, \tilde{i}) |H| dH d\tilde{e} d\tilde{i}, \quad (C4)$$

where $\psi(\tilde{e}, \tilde{i})$ is a distribution function of eccentricities and inclination for which we assume a Gaussian form (3) following Paper II, and N is dimensionless. The approach velocity of accreting planetesimals is [equation (60) of Paper II]

$$v^2 = \Omega^2 R_H^2 [\tilde{e}^2 + \tilde{i}^2 - (3/4)(H')^2]. \quad (C5)$$

We have used H' in this formula because calculation of scattering in the two-body approximation uses values of the orbital parameters immediately before the encounter.

The accretor will absorb all planetesimals which have impact parameters at infinity l smaller than

$$l_{max} = R_e \sqrt{1 + \frac{2G(M_e + m)}{R_e v^2}}, \quad (C6)$$

a condition from which (C2) follows. Then, using equation (A7) we may write that the fraction of δN which can get accreted is

$$f_a = P(H', l < l_{max}) = \frac{2}{3\pi} \frac{l_{max}^2}{R_H^2} \frac{v}{\Omega R_H} \frac{1}{\tilde{i} |H'| \sqrt{\tilde{e}^2 - (H')^2}}. \quad (C7)$$

Then the mass accretion rate due to the population of field particles with mass m is

$$\begin{aligned} \dot{M} &= m \int_{-\infty}^{\infty} dH \int_{|H|}^{\infty} \int_0^{\infty} d\tilde{e} d\tilde{i} \psi(\tilde{e}, \tilde{i}) f_a \frac{d\delta N}{dH} \\ &= m \frac{\Omega R_e^2}{\pi a_e^2} \int_{-\infty}^{\infty} dH \int_{|H|}^{\infty} \int_0^{\infty} N(H) \tilde{v}_0 \frac{|H|}{|H'|} \frac{\psi(\tilde{e}, \tilde{i}) d\tilde{e} d\tilde{i}}{\tilde{i} \sqrt{\tilde{e}^2 - (H')^2}} \left[1 + \frac{2}{p \tilde{v}_0^2} \right], \end{aligned} \quad (C8)$$

where we are using the following notation: $\tilde{v}(e, i) = v/(\Omega R_H)$, and p is given by (C1).

We carry out the integration over $d\tilde{e}$ and $d\tilde{i}$ in a way similar to our calculation of scattering coefficients in Appendix A of Paper II. As a result we obtain equations (42) and (43). Note that (42) automatically takes into account the transition between strong and weak gravitational focussing regimes which takes place at $\tilde{\sigma}_e, \tilde{\sigma}_i \sim p^{-1/2} \gg 1$. We have numerically compared (42) applied to a homogeneous planetesimal disk (and $H' = H$) with the corresponding analytical accretion rates of Greenzweig & Lissauer (1992) and found them to agree. The conversion between H' and H turns out to be a significant ingredient for the accuracy of the accretion rates; the use of simple $H' = H$ prescription instead of (27) leads to $\approx (10 - 20)\%$ bigger discrepancy with our numerical results.

In the shear-dominated regime [“intermediate dispersion, strong gravity” case of Dones & Tremaine (1993)] the situation is different. The approach velocity of planetesimals is always $\sim \Omega R_H$. Then the mass accretion rate can depend on only the vertical (and not horizontal) velocity dispersion since $\tilde{\sigma}_i$ determines the disk thickness and local density of planetesimals. Using simple scaling arguments and orbit integrations to fix constant coefficients Dones & Tremaine (1993) have demonstrated that in the shear-dominated regime with the ratio of vertical to horizontal velocity dispersions $\tilde{\sigma}_i/\tilde{\sigma}_e = 0.5$ the accretion rate in homogeneous disk is given by

$$\dot{M} \simeq 5 \frac{Nm\Omega R_e R_H}{\tilde{\sigma}_i a_e^2}. \quad (\text{C9})$$

In our case this result is no longer applicable because planetesimal surface density is not the same in different parts of the disk. In fact, when computing the accretion rate in inhomogeneous disk it is more meaningful to use *instantaneous* surface number density of planetesimals on passing orbits which lead to collisions with the embryo. We will assume that planetesimals on orbits near the horseshoe-passing boundary end up colliding with the embryo in the cold regime [see Petit & Hénon (1986) for more accurate locations of collision bands in the shear-dominated regime]; this means that we will be using the instantaneous surface density $N^{inst}(H_{coll})$ where $H_{coll} \approx \pm 1.4$ [see (20)] as a measure of surface density in equation (C9). Using results of Paper II (Appendix B) we can write that

$$N^{inst}(H_{coll}) = \frac{1}{\sqrt{2\pi}} \int_{-\infty}^{\infty} N(H) \frac{dH}{\tilde{\sigma}_e(H)} \exp \left[-\frac{(H - H_{coll})^2}{2\tilde{\sigma}_e^2(H)} \right]. \quad (\text{C10})$$

All these considerations allow us to adopt formula (44) for the accretion rate in the inhomogeneous disk with arbitrary ratio of vertical to horizontal planetesimal velocity dispersions. Of course, in the homogeneous disk with $\tilde{\sigma}_i/\tilde{\sigma}_e = 0.5$ it reproduces (C9).

In the intermediate velocity regime we smoothly interpolate between the accretion rates represented by formulae (44) and (42), see Appendix B. To compute the accretion rate in a disk with a distribution of planetesimal masses one simply needs to integrate our single-mass formulae over the whole planetesimal mass spectrum.